NASA TECHNICAL NOTE

NASA TN D-5992

NASA TN D-5992

AN ANALYSIS OF THE CAPABILITIES AND LIMITATIONS OF TURBINE AIR COOLING METHODS

by Jack B. Esgar, Raymond S. Colladay, and Albert Kaufman

Lewis Research Center
Cleveland, Ohio 44135

NATIONAL AERONAUTICS AND SPACE ADMINISTRATION • WASHINGTON, D. C. • SEPTEMBER 1970

1. Report No. NASA TN D-5992	2. Government Accession No.	3. Recipient's Catalog No.
4. Title and Subtitle AN ANALYSIS OF THE CAPABILITIES AND LIMITATIONS OF TURBINE AIR COOLING METHODS		5. Report Date September 1970 6. Performing Organization Code
7. Author(s) Jack B. Esgar, Raymond S. Colladay, and Albert Kaufman		8. Performing Organization Report No. E-5669
9. Performing Organization Name and Address Lewis Research Center National Aeronautics and Space Administration Cleveland, Ohio 44135		10. Work Unit No. 720-03 11. Contract or Grant No.
12. Sponsoring Agency Name and Address National Aeronautics and Space Administration Washington, D.C. 20546		13. Type of Report and Period Covered Technical Note 14. Sponsoring Agency Code
15. Supplementary Notes		

16. Abstract

The relative merits of convection, transpiration, and full coverage film air cooling methods were investigated for local turbine inlet temperatures from 2000° to 3500° F (1367 to 2200 K), gas pressures from 5 to 40 atmospheres (50.7 to 405.3 N/cm^2), and cooling air temperatures from 600° to 1200° F (589 to 922 K). Effects of blade and vane wall thickness, leading edge radius, and material temperature were also investigated. The results indicate the design trends required for the cooled turbines of future engines, the superiority of transpiration and full coverage film cooling over convection cooling, and approaches that can be used to improve convection cooling.

17. Key Words (Suggested by Author(s))	18. Distribution Statement
Turbine cooling Heat Transfer	Unclassified - unlimited

19. Security Classif. (of this report)	20. Security Classif. (of this page)	21. No. of Pages	22. Price*
Unclassified	Unclassified	51	$3.00

*For sale by the Clearinghouse for Federal Scientific and Technical Information
Springfield, Virginia 22151

AN ANALYSIS OF THE CAPABILITIES AND LIMITATIONS OF TURBINE AIR COOLING METHODS

by Jack B. Esgar, Raymond S. Colladay, and Albert Kaufman

Lewis Research Center

SUMMARY

An analytical investigation was conducted to determine the relative merits of convection, transpiration, and full coverage film air cooling methods for local turbine inlet temperatures from 2000° to 3500° F (1367 to 2200 K), gas pressures from 5 to 40 atmospheres (50.7 to 405.3 N/cm^2), and cooling air temperatures from 600° to 1200° F (589 to 922 K). Effects of blade and vane wall thickness, leading edge radius, and material temperature were also investigated.

It was determined that convection cooling becomes extremely difficult under the high heat flux conditions that result from high gas temperatures and pressures. Reducing the wall thickness or utilizing materials with considerably higher temperature limitations can significantly increase the range of conditions under which convection cooling will be satisfactory. Convection cooled stators for local turbine inlet temperatures to 3500° F (2200 K) are possible with a material temperature of 2200° F (1478 K).

Increasing allowable metal temperature 100° F (56 K) or reducing cooling air temperature 200° F (111 K) can do more to improve the cooling capabilities of convection cooled blades and vanes than is possible by improvements in the better state-of-the-art convection designs.

The coolant flow requirements for full coverage film and transpiration cooling are very much lower than for convection cooling at high turbine inlet temperatures and high compressor pressure ratios. These cooling methods can often permit turbine inlet temperatures 1000° F (556 K) higher than permitted with convection cooling at the same coolant flow ratio. Cooling air temperature and maximum allowable wall temperature have considerably less effect on the coolant flow requirements for transpiration and full coverage film cooling than for convection cooling.

Oxidation of presently available transpiration cooled materials requires a material temperature reduction relative to other cooling methods so that for many applications transpiration cooling requires more coolant flow than full coverage film cooling. Recent research on transpiration cooling materials shows promise of allowing material temperatures that will make coolant flow requirements for transpiration cooling less than that for other cooling methods at nearly all gas temperature levels.

INTRODUCTION

An analysis was conducted to determine the potentials of convection, full coverage film, and transpiration cooling for ranges of turbine inlet temperature and compressor pressure ratio expected in future gas turbine engines.

It is necessary to review periodically the expected future trends for gas turbine engines and then determine how these trends will affect the necessary research and development work in the various engine components. The trend in both military and commercial gas turbine engines is towards turbofan engines having a compact, high temperature gas generator. To make such engines compact, lightweight, and with superior specific fuel consumption, there is the need to simultaneously increase both compressor pressure ratio and turbine inlet temperature. Compressor pressure ratios to 40 or higher appear to be looming in the future, and turbine inlet temperatures may go to those corresponding to stoichiometric fuel-air mixtures if materials and cooling designs can be developed that will tolerate such temperatures reliably.

Up to the present time convection cooling has been the primary means of cooling gas turbine engines, with some film cooling augmentation in critical regions. At the severe cooling conditions expected in future engines, it is likely that convection cooling will be inadequate, and more advanced cooling schemes such as film and transpiration cooling will have to be utilized. In reference 1 it was shown that the potentials of convection cooling could be determined in a relatively simple manner by considering the blades as heat exchangers and evaluating the cooling requirements on a basis of the heat capacity of the cooling air flowing through the blades and vanes. Research being conducted on transpiration and film cooling methods is reported in references 2 to 10.

In order to evaluate the relative potentials of convection, film, and transpiration cooling for future engines, analyses were made of expected heat fluxes that will be encountered in future engines for ranges of gas pressures from 5 to 40 atmospheres (50.7 to 405.3 N/cm^2) and for local turbine inlet temperatures from 2000° to 3500° F (1367 to 2200 K). Required coolant flows were then calculated for turbine rotor blades and stator vanes and compared relative to those needed for advanced convection cooled vanes and blades at a turbine inlet temperature of 2500° F (1644 K). Parameters investigated included cooling air temperature from 600° to 1200° F (589 to 922 K), blade and vane maximum metal external surface temperatures from 1400° to 2400° F (1033 to 1589 K), blade and vane wall thicknesses from 0.020 to 0.050 inch (0.51 to 1.27 mm), and leading edge diameters from 0.20 to 0.40 inch (5.08 to 10.16 mm).

ANALYTICAL PROCEDURE

In order to make the results of this investigation be of a general nature rather than

for a specific application, very few assumptions were made that would restrict the result to applications for any specific engine, but some specific assumptions were required. These assumptions are given in table I.

TABLE I. - ASSUMPTIONS USED IN ANALYSIS

Condition	Stator	Rotor
Gas approach Mach number	0.24	0.5
Average gas channel Mach number	0.60	0.65
Airfoil chord, in. (cm)	2.0 (5.08)	1.5 (3.81)
Ratio of relative gas total temperature to stator inlet total temperature	1.0	0.9
Ratio of relative gas total pressure to stator inlet total pressure	1.0	0.7
Metal thermal conductivity for convection cooling, Btu/(hr)(ft)(^{o}F) (J/(m)(sec)(K))	12 (20.75)	12 (20.75)
Effective metal thermal conductivity for film cooling, Btu/(hr)(ft)(^{o}F) (J/(m)(sec)(K))	11 (19.03)	11 (19.03)
Effective porous metal thermal conductivity for transpiration cooling (ref. 11), Btu/(hr)(ft)(^{o}F) (J/(m)(sec)(K))	8 (13.84)	8 (13.84)

Cooling air temperature is influenced by compressor pressure ratio, flight speed, flight altitude, and whether the temperature has been reduced by rejecting heat to fuel or engine bypass air. As a result, no attempt has been made to consistently vary cooling air temperature with total gas pressure.

Heat-Transfer Models

Figure 1 illustrates the three heat-transfer models used in analyzing the coolant requirements for convection, full coverage film, and transpiration cooled turbine blades and vanes. Figure 1(a) illustrates in schematic form one of the many heat-transfer models that can be used for convection cooling. With this cooling method, all of the heat transferred from the gas to the blade or vane must be conducted through the wall before it can be transferred to the cooling air by convection. As a result, the temperature drop through the wall, due to conduction, decreases the driving temperature difference between the wall and the coolant. The thermal effectiveness of the cooling air is then defined as

$$\eta_{conv} = \frac{T_{c,o} - T_{c,i}}{T_{B,i} - T_{c,i}} \tag{1}$$

(All symbols are defined in appendix A.) For the analyses of this report, calculations were made for values of thermal effectiveness η_{conv} equal to 0.5, 0.7, and 1.0.

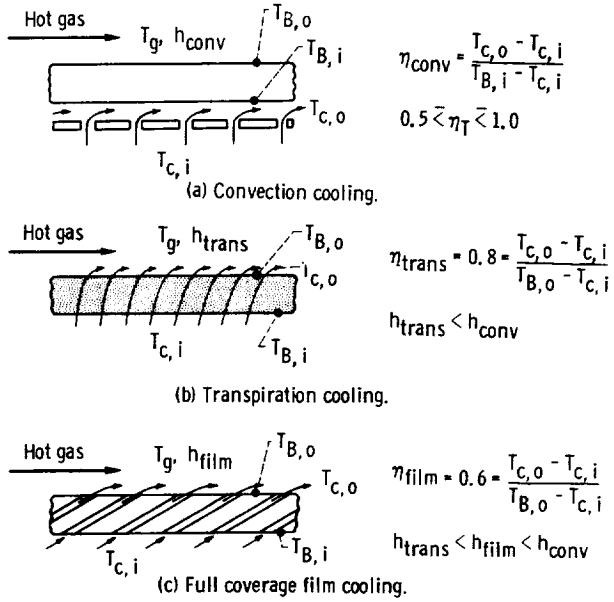

Figure 1. - Heat-transfer models used in analysis.

Figure 1(b) illustrates the heat-transfer model used for the transpiration cooling analysis. With transpiration cooling, the coolant is still in contact with the wall on the outer (hottest) surface. As a result, this cooling scheme has the potential of heating the cooling air to a higher temperature than is possible with convection cooling. Therefore, for transpiration cooling the equation for thermal effectiveness of the cooling air

$$\eta_{trans} = \frac{T_{c,o} - T_{c,i}}{T_{B,o} - T_{c,i}} \tag{2}$$

has the value $T_{B,o}$ in the denominator instead of $T_{B,i}$ as was in equation (1) for convection cooling. The value of $\eta_{trans} = 0.8$ is an assumed value that will be discussed in more detail later.

In addition, the gas-to-blade heat-transfer coefficient for transpiration cooling is reduced relative to convection cooling by the layer of boundary layer air that is devel-

oped by transpiration as discussed in references 6 to 10. A transpiration cooled blade or vane will, therefore, have less heat transferred to it from the gas than a convection cooled blade or vane.

Figure 1(c) illustrates the full coverage film cooling heat-transfer model. This type of film cooling resembles transpiration cooling except there are fewer (and larger) holes for the cooling air to pass through to the outside surface. Full coverage film cooling provides a layer of air on the outside surface of the blade or vane that reduces the gas-to-blade heat-transfer coefficient relative to convection cooling, but to a lesser degree than for transpiration cooling. In the analysis conducted in this report, the full coverage film cooling model was considered to approach maximum usefulness of film cooling by providing a very large number of small film cooling passages. The equation for thermal effectiveness η_{film} for film cooling is the same as equation (2) for transpiration cooling, but the value of thermal effectiveness ($\eta_{film} = 0.6$) was assumed to be lower, as will be discussed in more detail later. With film cooling, depending on the configuration, the heating of the cooling air could all occur within the film cooling passages, or part of the heating could result from convection cooling on the inside surface prior to the cooling air entering the film cooling passages.

Convection Cooling Analysis

For convection cooling under steady-state conditions the following one-dimensional heat-transfer equations are applicable:

Hot gas to outside surface:

$$\frac{Q}{A} = h_{conv}(T'_g - T_{B,o}) \tag{3}$$

Conduction through the wall:

$$\frac{Q}{A} = \frac{k_B}{t}(T_{B,o} - T_{B,i}) \tag{4}$$

Heat picked up by cooling air:

$$\frac{Q}{A} = \frac{w_c c_{p,c}}{A}(T_{c,o} - T_{c,i}) \tag{5}$$

Combining equations (1), (3), (4), and (5) results in

$$\frac{w_c c_{p,c}}{A} = \frac{h_{conv}}{\eta_{conv}} \left[\frac{T'_g - T_{B,o}}{T_{B,o} - \frac{h_{conv} t}{k_B} (T'_g - T_{B,o}) - T_{c,i}} \right] \tag{6}$$

Equations (3) and (6) contain the term for relative total gas temperature T'_g. To be more exact, this term should be the adiabatic wall temperature, sometimes called the effective gas temperature. For subsonic relative velocities the effective gas temperature is within 1 or 2 percent of the relative total gas temperature. For the purpose of this investigation, use of the relative total gas temperature was accurate enough.

Gas-to-surface heat-transfer coefficient (aft of leading edge). - It was assumed that aft of the leading edge the boundary layer was turbulent and the average heat-transfer coefficient could be calculated by the flat plate equation of reference 12:

$$\bar{h}_{conv} = 0.037 \, Re^{0.8} Pr^{1/3} \frac{k}{L} \tag{7}$$

where the characteristic dimension L is the surface length of the blade or vane measured from the leading edge. Values of L used in the calculations were 2 inches (5.08 cm) for stator vanes and 1.5 inches (3.81 cm) for rotor blades. The fluid properties in equation (7), including the temperature effect on density, were evaluated at the reference temperature given in reference 12:

$$T_{ref} = 0.5 \, T_{B,o} + 0.28 \, T_g + 0.22 \, T_e \tag{8}$$

where

$$T_e = T_g + \Lambda(T'_g - T_g) \tag{9}$$

$$\Lambda = Pr^{1/3} \tag{10}$$

The fluid properties, Pr, thermal conductivity, ratio of specific heats, and viscosity, were obtained from the charts in reference 13 for ASTM-A-1 fuel and a pressure of 10 atmospheres.

Combining equation (7) with gas channel Mach number pressure and temperature relations for a constant Prandtl number of 0.705 results in

$$\bar{h}_{conv} = 0.033 \frac{k}{L} \left[\frac{p'ML \sqrt{\frac{\gamma g T'_g}{R}}}{\mu T_{ref} \left(1 + \frac{\gamma - 1}{2} M^2\right)^{(3\gamma-1)/2(\gamma-1)}} \right]^{0.8} \tag{11}$$

Gas-to-surface heat-transfer coefficient (leading edge stagnation). - From reference 14 the local heat-transfer coefficient for a cylinder in cross flow can be determined from

$$h_{conv} = 1.14 \frac{k}{D} Re^{1/2} Pr^{0.4} \left[1 - \left(\frac{\varphi}{90}\right)^3\right] \tag{12}$$

Because this equation was used for high velocity gas flow the gas properties were based on the reference temperature given in equation (8), and the laminar flow recovery factor Λ was taken as

$$\Lambda = \sqrt{Pr} \tag{13}$$

In a manner similar to that described for equation (11), and for $\varphi = 0$ (stagnation point), the local stagnation point heat-transfer coefficient can be written

$$h_{conv} = 0.992 \frac{k}{D} \left[\frac{p'MD \sqrt{\frac{\gamma g T'_g}{R}}}{\mu T_{ref} \left(1 + \frac{\gamma - 1}{2} M^2\right)^{(3\gamma-1)/2(\gamma-1)}} \right]^{1/2} \tag{14}$$

Cooling air thermal effectiveness. - Data from reference 1 are shown in figure 2 to illustrate the range of cooling air thermal effectiveness

$$\eta_{conv, avg} = \frac{T_{c,o} - T_{c,i}}{T_{B,avg} - T_{c,i}}$$

that can be expected for a range of relatively sophisticated convection cooled turbine blades designed for a supersonic aircraft engine at cruise conditions (gas pressure of 3.5 atm or 35.4 N/cm^2). It is seen that these blades have thermal effectiveness values ranging from slightly more than 0.5 to about 0.8. If the inside wall temperature $T_{B,i}$ had been used in defining this effectiveness (as in eq. (1)) instead of the average wall

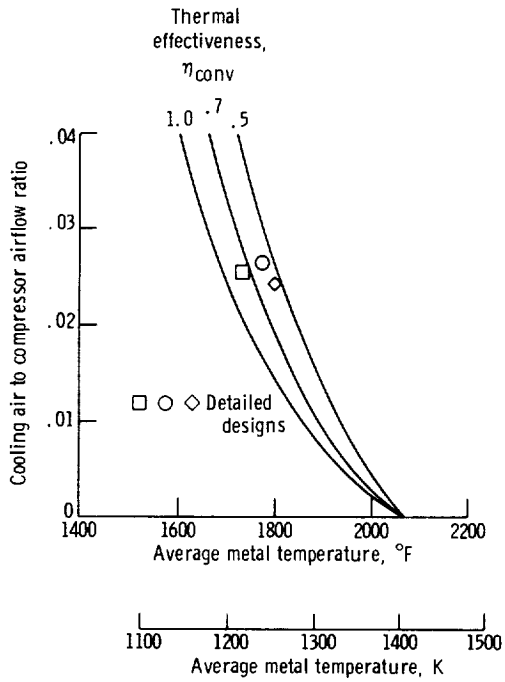

Figure 2. - Heat exchanger effectiveness of air cooled turbine blades (ref. 1). Cooling air thermal effectiveness, $\eta_{conv,avg} = (T_{c,o} - T_{c,i})/(T_{B,avg} - T_{c,i})$.

temperature $T_{B,avg}$, the values of η_{conv} would have been slightly higher (less than 5 percent). The effect is small in this case since the heat fluxes in reference 1 were low enough that the difference between $T_{B,i}$ and $T_{B,avg}$ was low (on the order of 35° F (19 K)).

The value of η_{conv} is not a constant for a given convection cooling configuration. It decreases as the cooling airflow (Reynolds number) increases. Therefore η_{conv} will be smaller for the more difficult cooling conditions of high gas pressure and temperature. The dependence of η_{conv} on Reynolds number is shown from the following simple analysis. The heat transferred to the cooling air is

$$\frac{Q}{A_i} = h_c(T_{B,i} - T_{c,i})$$

Combining this equation with equations (1) and (5) results in

$$\eta_{conv} = \frac{h_c A_i}{w_c c_{p,c}}$$

which can be written

$$\eta_{conv} = \frac{Nu_c}{Re_c Pr_c} \frac{A_i}{A_f}$$

For turbulent heat transfer and a constant cooling air Prandtl number

$$Nu_c \propto Re_c^{0.8}$$

Therefore,

$$\eta_{conv} \propto \frac{1}{Re^{0.2}}$$

In the analysis of this report the cooling air Reynolds numbers could range up to 16 times the value for the conditions of figure 2. Such Reynolds numbers could result in a reduction of η_{conv} by a factor of as much as 1.74. The maximum value of η_{conv} in figure 2 was about 0.8. Dividing this number by 1.74 could result in η_{conv} values as low as 0.46.

Most relative coolant flow ratios for convection cooling presented in this report are for a value of $\eta_{conv} = 0.7$. The value of relative coolant flow ratio for convection cooling corresponding to any other value of η_{conv} can be obtained very simply by multiplying the relative coolant flow ratio read from the curves of this report by the ratio $0.7/\eta_{conv}$. For the analyses of this report, values of 0.5, 0.7, and 1.0 were taken for cooling air thermal effectiveness to show the range possible with convection cooling, while 0.7 was taken as a value that represents advanced, but possible, cooling designs. A value of $\eta_{conv} = 1.0$ is the ideal case and represents a limit to the amount of cooling that is possible with convection.

Transpiration Cooling Analysis

With transpiration cooling the heat-transfer analysis approach was similar to that for convection cooling except the inside wall temperature does not provide a restriction on the temperature rise of the cooling air. The following one-dimensional heat-transfer equations are applicable:

Hot gas to outside surface:

$$\frac{Q}{A} = h_{conv} \frac{h_{trans}}{h_{conv}} (T'_g - T_{B,o}) \tag{15}$$

Heat picked up by cooling air:

$$\frac{Q}{A} = \frac{w_c c_{p,c}}{A} (T_{c,o} - T_{c,i}) \tag{5}$$

Combining equations (2), (5), and (15) results in

$$\frac{w_c c_{p,c}}{A} = \frac{h_{conv}}{\eta_{trans}} \frac{h_{trans}}{h_{conv}} \frac{T'_g - T_{B,o}}{T_{B,o} - T_{c,i}} \tag{16}$$

The reduction in gas-to-wall heat-transfer coefficient with transpiration cooling has been determined experimentally in references 6 to 10 and the results agree with the following relation developed in references 15 and 16:

$$\frac{St_{trans}}{St_{conv}} = \frac{B}{e^B - 1} \tag{17}$$

where

$$B = \frac{\frac{\rho_c V_c}{\rho_g V_g}}{St_{conv}} \tag{18}$$

$$B = \frac{\rho_c V_c c_{p,g}}{h_{conv}} \tag{19}$$

The Stanton number ratio (eq. (17)) is equal to the ratio of heat-transfer coefficients. Noting that $\rho_c V_c = w_c/A$, equations (17) and (19) can be rewritten

$$\frac{h_{trans}}{h_{conv}} = \frac{B}{e^B - 1} \tag{17a}$$

$$B = \frac{w_c c_{p,c}}{A} \frac{c_{p,g}}{c_{p,c}} \frac{1}{h_{conv}} \tag{19a}$$

The required coolant flow for a transpiration cooled surface can be obtained by combining equations (16), (17a), and (19a) to yield

$$\frac{w_c c_{p,c}}{A} = h_{conv} \frac{c_{p,c}}{c_{p,g}} \ln\left[\frac{1}{\eta_{trans}} \frac{c_{p,g}}{c_{p,c}} \left(\frac{T'_g - T_{B,o}}{T_{B,o} - T_{c,i}}\right) + 1\right] \tag{20}$$

The value of η_{trans} in equation (20) was assumed to be 0.8. It is more frequently assumed that the cooling air discharges from a transpiration cooled surface at the same temperature as the outside wall temperature, which would result in $\eta_{trans} = 1.0$. Based on the fact that transpiration cooled walls in gas turbine engines will be thin (about 0.030 to 0.050 inch (0.76 to 1.27 mm)) with a limited amount of internal (within the wall) surface area in contact with the coolant, it seems unlikely that $\eta_{trans} = 1.0$ is a good assumption. The value of 0.8 appears to offer some conservatism to the analysis.

Full Coverage Film Cooling Analysis

To obtain maximum cooling effectiveness from film cooling, the holes should be closely spaced over the entire surface in order to generate complete film coverage over the surface. Such a cooling scheme approaches transpiration cooling, but it is less effective than transpiration cooling because (1) a finite number of film cooling holes will not provide as uniform an insulating film of cooling air on the outside surface as the almost infinite number of holes obtained by transpiration cooling, and (2) transpiration cooling can utilize more of the heat capacity in the cooling air for reducing wall temperature by internal convection within the walls due to the very large surface area in contact with the coolant relative to film cooling.

Most film cooling analyses, such as those in references 2 and 5, are for isolated holes or for rows of holes. These investigations and others have utilized several different methods of accounting for the method of heat transfer by film cooling. Frequently, it is assumed that the gas-to-surface heat-transfer coefficient is the same as with convection, but the effective gas temperature is reduced by the insulating effect of the film. Some investigators have considered a reduction in gas-to-surface heat-transfer coefficient due to film cooling. Since the model assumed in the present investigation has a large number of holes, which approaches transpiration cooling, a modified transpiration cooling analysis was used herein to calculate the cooling air requirements for full cover-

age film cooling.

It was assumed that the gas-to-surface heat-transfer coefficient for full coverage film cooling would be a value midway between that for transpiration cooling and convection cooling and that the film cooling thermal effectiveness η_{film} would be equal to 0.6.

From the limited information available, both of these assumptions are conservative based on the potential of full coverage film cooling techniques. The calculation procedure for full coverage film cooling was similar to that for transpiration cooling except equation (16) was replaced by

$$\frac{w_c c_{p,c}}{A} = \frac{h_{conv}}{\eta_{film}} \frac{h_{film}}{h_{conv}} \frac{T'_g - T_{B,o}}{T_{B,o} - T_{c,i}} \tag{21}$$

and equation (17a) was replaced by

$$\frac{h_{film}}{h_{conv}} = \frac{1}{2}\left(1 + \frac{h_{trans}}{h_{conv}}\right) \tag{22}$$

where h_{trans}/h_{conv} was calculated from equation (17a) for the value of coolant flow from equation (21). This procedure required iteration of equations (17a), (19a), (21), and (22).

Temperature Drop Through Wall

For convection cooling the steady-state temperature drop through the wall is linear. The temperature drop through the wall can be calculated by combining equations (3) and (4) to yield

$$T_{B,o} - T_{B,i} = \frac{h_{conv} t}{k_B} (T'_g - T_{B,o}) \tag{23}$$

The temperature distribution through transpiration cooled and advanced film cooled walls can be calculated by the method derived in appendix B. The temperature drop through these walls is obtained from the following equations developed in appendix B:

$$T_{B,o} - T_{B,i} = T_{B,o} - (C_2 + C_3) \tag{24}$$

where

$$C_2 = \frac{\left(a_2 - \frac{\lambda}{\beta}\eta\right)}{(a_2 - a_1)e^{a_1}}$$

$$C_3 = -\frac{\left(a_1 - \frac{\lambda}{\beta}\eta\right)}{(a_2 - a_1)e^{a_2}}$$

$$a_1 = -\frac{1}{2}\left(\beta + \sqrt{\beta^2 + 4\lambda}\right)$$

$$a_2 = -\frac{1}{2}\left(\beta - \sqrt{\beta^2 + 4\lambda}\right)$$

$$\lambda = \frac{h_i \sigma t^2}{k_B}$$

$$\beta = \frac{h_i \sigma t A}{w_c c_{p,c}}$$

$$\sigma = \frac{\Delta A_i}{A\,\Delta x} = \frac{\text{internal surface area}}{\text{volume}}$$

Blade Life

The analysis for blade life was based on the geometry of a typical first stage rotor blade with a centrifugal stress of the airfoil shell at the root section of 26 000 pounds per square inch (179 N/mm^2) at cruise. Blade lives were also evaluated for a centrifugal stress 50 percent greater (39 000 lb/in.^{2} (269 N/mm^2)). Lives were calculated for through-the-wall temperature drops of 48°, 300°, 480°, and 600° F (27, 167, 267, and 333 K). These linear wall temperature drops were assumed constant over the whole airfoil perimeter. The outer surface of the blade was held constant at an oxidation limiting temperature of 1800° F (1255 K).

The shell section was divided into a total of 245 nodes or area elements with 12 rows of nodes through the wall. At the trailing edge there were from 19 to 22 nodes through

the wall because of the increased thickness. The blade was assumed to be fabricated from cast IN 100 (15Co-10Cr-5.5Al-4.7Ti-3Mo-Ni). Creep data and stress rupture data from reference 17 and stress-strain and strain cycling fatigue data from reference 18 were used in conjunction with the stress relaxation program described in reference 19 to determine the blade lives.

A detailed explanation of the procedure for combining the effects of fatigue and steady-state creep damage is presented in reference 20. Briefly, this method consists of the following steps: (1) determine the relaxed stress level at each node; (2) compute the times to stress rupture at the most critical nodes based on both the relaxed stresses and the accelerated creep damage before relaxation as explained in reference 20; (3) compute the number of cycles to fatigue failure based on the total strains at these nodes and strain cycling data; and (4) combine the effects of creep and fatigue damage by a life-fraction rule which assumes that the percent of the total damage due to each of these failure mechanisms must add up to 100 percent. Since the heat-transfer analysis did not consider transient effects, the total strains at the initial conditions (zero hr at steady-state cruise) were assumed equivalent to the total strain changes. The stress relaxation will affect the total strain levels but not the total strain changes per engine cycle as demonstrated in reference 20. Stress concentration effects due to film cooling holes were taken into account by using strain cycling data for bar specimens with holes (ref. 18). It was assumed that the aircraft would undergo a 2-hour cruise flight and, therefore, each cycle was equivalent to 2 hours of steady-state operation.

RESULTS AND DISCUSSION

This report indicates the cooling potential and limitations for convection, transpiration, and full coverage film cooling, and it compares the cooling airflow requirements for each of these methods. Attempts were made to not be unduly optimistic about the gains that can be obtained with the less studied transpiration and full coverage film cooling compared to the more conventional convection cooling method. The assumptions used in this analysis have favored convection cooling to an extent probably not found in the present state-of-the-art, and except for possible effects of gas stream turbulence, the assumptions have probably penalized transpiration and full coverage film cooling.

For most convection cooling comparisons, the cooling air thermal effectiveness η_{conv} was assumed to be 0.7, a high value found only in advanced convection cooled configurations at heat fluxes corresponding to relatively low gas pressures and temperatures. Experimental evidence indicates that $\eta_{conv} = 0.7$ is difficult to obtain and a value of 0.5 is probably more realistic, particularly at high gas temperatures and pressures. For transpiration cooling, experimental data have indicated that the cooling air

thermal effectiveness η_{trans} can be equal to 1. This analysis assumed a conservative value of only 0.8. Data for full coverage film cooling are much more limited than for the other two cooling methods. Limited experimental data have indicated that the assumed value of cooling air thermal effectiveness $\eta_{film} = 0.6$ is a conservative assumption.

The combustion process in turbine engines creates high turbulence levels in the gas stream. Most experimental heat-transfer investigations are conducted at low turbulence levels. The effects of this turbulence on heat-transfer processes has not been adequately investigated. It is not known whether the effects on transpiration and film cooling will be greater or less than those for convection cooling. Turbulence can cause hot gas mixing with the insulating blanket of cooling air generated by transpiration and film cooling and reduce their effectiveness. This turbulence effect has not been considered in the present analysis since experimental data are lacking, but all other assumptions have been stacked in favor of convection cooling. The results show a marked superiority for transpiration and full coverage film cooling over convection cooling.

Relative Coolant Flow Requirements

An approximate analysis, such as the one in this report, does more to indicate trends than absolute values of coolant flow that are required for various cooling methods. The analysis compares convection, full coverage film, and transpiration cooling based on cooling air thermal effectiveness η. Such an approach can be useful, but its limitations must also be considered. As previously discussed, it is probably not possible to obtain the same values of cooling air thermal effectiveness for all cooling conditions because of the variations in cooling air Reynolds number, which result from variations in temperature and pressure level of the gas and coolant and the temperatures of the blade or vane material.

This report compares the various cooling conditions and cooling methods on the basis of "relative coolant flow ratio." Coolant flow ratio is defined as the ratio of cooling airflow to compressor airflow. Relative coolant flow ratio is the coolant flow ratio relative to a "base" flow for a specific convection cooled blade or vane. In this report the coolant flows are per unit of blade or vane surface area. The base flows have a compensation for gas pressure level. This compensation accounts for variations in compressor airflow with pressure level. No attempt was made to apply a similar compensation for variations in compressor airflow resulting from gas temperature level since such a compensation would be small relative to the compensation for pressure.

For a comparison of the effects of gas, coolant, and material temperature, material thickness, and leading edge diameter at a constant gas pressure of 20 atmospheres (202.6 N/cm^2), the "base" coolant flow used to calculate the "relative coolant flow

ratio" is that required for the same location on a blade or vane of an advanced state-of-the-art convection cooled blade or vane ($\eta_{conv} = 0.7$) at the following conditions: (1) total gas pressure at the stator inlet of 20 atmospheres (202.6 N/cm^2), (2) turbine inlet temperature of 2500^o F (1644 K), (3) cooling air temperature of 1000^o F (811 K), (4) blade or vane wall thickness of 0.050 inch (1.27 mm), and (5) material temperatures consistent with present practice - 1700^o F (1200 K) for aft sections of rotor blades, 1800^o F (1255 K) for aft sections of stator vanes and rotor blades leading edges, and 2000^o F (1367 K) for stator vane leading edges).

For gas pressures different from 20 atmospheres (202.6 N/cm^2) the "base" coolant flow in the relative coolant flow ratio at each pressure level has been assumed to be that which would result if the coolant side heat-transfer coefficient varied with gas pressure level in a manner exactly proportional to that for the gas side coefficient. All other conditions are the same as those listed previously for 20 atmospheres (202.6 N/cm^2). This method of comparison is believed to give a reasonable approximation of how the coolant flow ratio would have to be varied in an engine as design gas pressure is varied.

In this report, turbine inlet temperature is defined as the total gas temperature at the stator inlet. The relative total gas temperature at the rotor was assumed to be 90 percent of the turbine inlet temperature. This temperature reduction results from both hot gas dilution from stator cooling air and the relative temperature reduction due to rotation of the rotor.

Stator vanes, aft of leading edge. - Relative coolant flow ratio requirements are shown in figure 3 for the section of the stator vanes aft of leading edge for a range of local turbine inlet temperatures from 2000^o to 3500^o F (1367 to 2200 K) and cooling air temperatures from 600^o to 1200^o F (589 to 922 K) for convection, full coverage film, and transpiration cooling.

Since stator vanes must be designed for combustor outlet hot spots, the turbine inlet temperatures shown in the abscissas of figure 3 are local rather than average turbine inlet temperatures. The coolant flow requirements for convection cooling are shown for ranges of cooling air thermal effectiveness η_{conv} from 0.5 to 1.0. The plots in figure 3 were calculated for a gas pressure of 20 atmospheres (202.6 N/cm^2) and a maximum wall surface temperature of 1800^o F (1255 K).

Figure 3 shows that with turbine cooling air temperatures of 1000^o to 1200^o F (811 to 922 K), which are appropriate compressor discharge temperatures for compressor pressure ratios in excess of 20, convection cooling offers limited possibilities for raising local turbine inlet temperature much above 2500^o F (1644 K). It is obvious, therefore, that more advanced, and possibly complex, cooling methods will be required if the very high turbine inlet temperatures predicted for the future are to be obtained. Figure 3 shows that transpiration cooling and full coverage film cooling offer the potential for obtaining turbine inlet temperatures approaching those corresponding to stoichio-

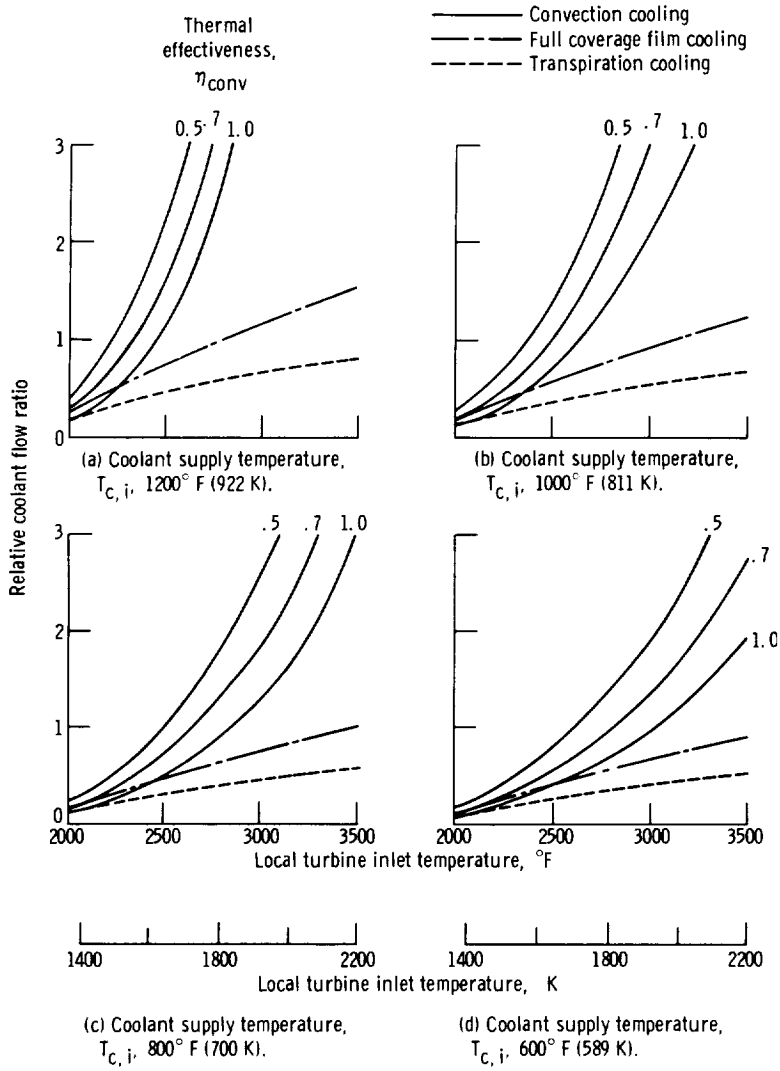

Figure 3. - Relative coolant flow requirements for aft section of stator vanes. Outside wall temperature, $T_{B,o}$, 1800° F (1255 K); wall thickness, t, 0.050 inch (1.27 mm); gas pressure, $p'_{g,s}$, 20 atmospheres (202.6 N/cm^2).

metric fuel-air mixture at reasonable coolant flow ratios. Transpiration and full coverage film cooling can often permit turbine inlet temperatures 1000° F (566 K) higher than permitted with convection cooling at the same coolant flow ratio.

The practical range of cooling air thermal effectiveness η_{conv} for effective convection cooled blades and vanes lies in the range from 0.5 to 0.7. Although there are significant benefits in increasing this thermal effectiveness above 0.7 by improved cooling configurations, reducing cooling air temperature provides a much greater leverage for reducing coolant flow requirements or to permit increasing turbine inlet temperature. Comparison of the plots in figure 3 for cooling air temperatures of 1000° F (811 K) and 800° F (700 K) shows the following:

(1) For a relative coolant flow ratio of 2.0 and a coolant temperature of 1000° F (811 K), the allowable local turbine inlet temperature is 2800° F (1811 K) for η_{conv} = 0.7. By going to the ultimate in convection cooling for η_{conv} = 1.0 the allowable local turbine inlet temperature could be increased to 2970° F (1906 K). If, however, the cooling air temperature were reduced to 800° F (700 K), the allowable local turbine inlet temperature could be increased to 3050° F (1950 K), which is 80° F (44 K) higher than would be possible with a "perfectly cooled" convection cooled vane.

(2) For a local turbine inlet temperature of 3000° F (1922 K) and a coolant temperature of 1000° F (811 K), the required relative coolant flow ratio is 3.0 for η_{conv} = 0.7. For η_{conv} = 1.0, the relative coolant flow ratio could be reduced to 2.1. However, reducing the cooling air temperature to 800° F (700 K) for η_{conv} = 0.7 reduces the required coolant flow ratio even further to 1.85.

The previous two comparisons show, therefore, that starting with an effective convection cooling configuration (η_{conv} = 0.7) it is far more beneficial to reduce cooling air temperature than to try to further improve the cooling effectiveness of the blades or vanes.

Rotor blades, aft of leading edge. - Figure 4 shows relative coolant flow requirements for first-stage turbine rotor blades in a manner similar to that for the stator vanes in figure 3. All of the coolant flow ratios in figure 4 are relative to those required for rotor blades of an advanced convection cooling design at a gas temperature of 2500° F (1644 K), a cooling air temperature of 1000° F (811 K), and an external surface metal temperature of 1700° F (1200 K).

Whereas stator vanes must be designed for the local combustor hot spot temperature, rotor blades are designed for the circumferentially averaged gas temperature at the critical radial location (based on stress and temperature). The effect of local combustor hot spots is averaged out by the rotation. Therefore the turbine inlet temperatures in the abscissas of figure 4 are circumferentially averaged temperatures at the stator inlet for the critical radial location, whereas the turbine inlet temperature in figure 3 are local hot spot values. The results shown can be applied with any combustor outlet temperature pattern. All the coolant flow ratios for stator vanes are relative to the requirements for a convection cooled vane, and rotor blade coolant flow ratios are relative to a convection cooled blade.

The trends shown in figures 3 and 4 are similar. It is interesting to note, however, that the coolant flow requirements for transpiration and film cooling are higher relative to convection cooling for rotor blades than for stator vanes. This effect is due to the fact that full coverage film and transpiration cooling become markedly superior to convection cooling at high heat fluxes resulting from high gas temperatures. Since the relative gas temperature for the rotor blade is from 250° to 400° F (139 to 222 K) less than the turbine inlet temperature, the rotor blade heat fluxes are not high enough to show as

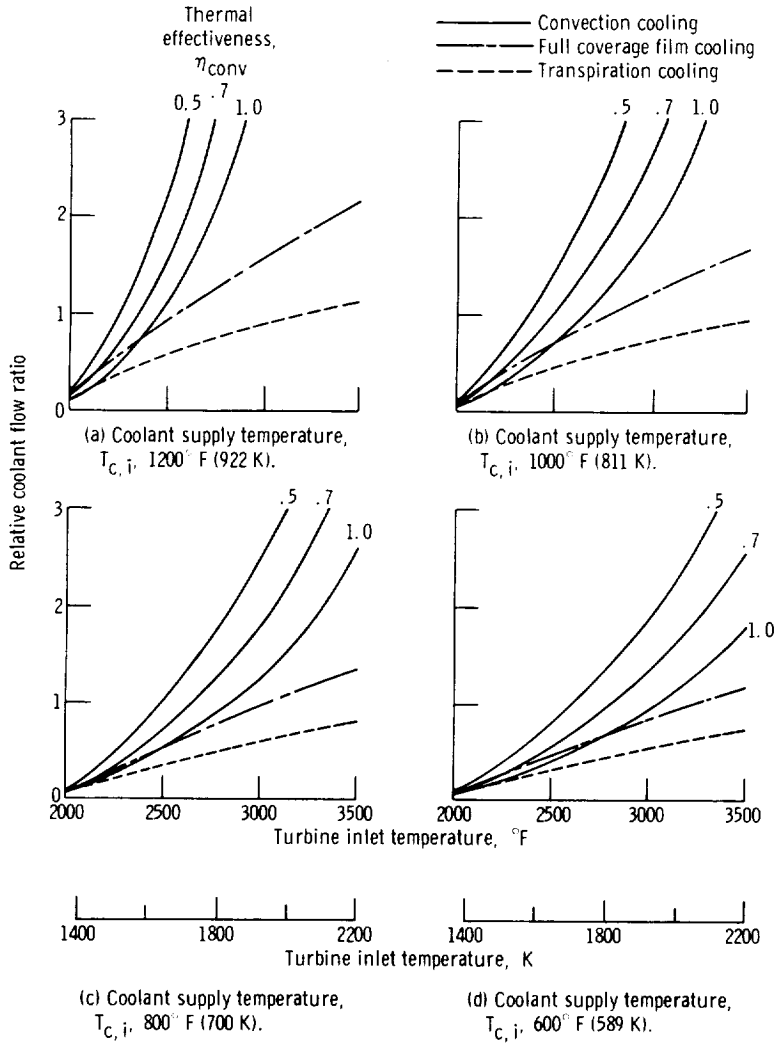

Figure 4. - Relative coolant flow requirements for aft section of rotor blades. Outside wall temperature, $T_{B,o}$, 1700° F (1200 K); wall thickness, t, 0.050 inch (1.27 mm); gas pressure, $p'_{g,s}$, 20 atmospheres (202.6 N/cm^2).

large relative coolant flow improvements for full coverage film and transpiration cooling for rotor blades as for stator vanes. The figure shows, however, that full coverage film or transpiration cooling will probably be required for rotor blades for turbine inlet temperatures very much in excess of 2500° F (1644 K) unless cooling air temperature can be reduced to values less than 1000° F (811 K).

Leading edge. - Figure 5 shows the relative coolant flow requirements for the leading edge section of the first-stage stator vanes for a gas pressure of 20 atmospheres (202.6 N/cm^2). Figure 5(a) shows the cooling requirements for a leading edge with a maximum surface temperature of 2000° F (1367 K) for convection, full coverage film, and transpiration cooling. The convection cooling results have a cooling air thermal

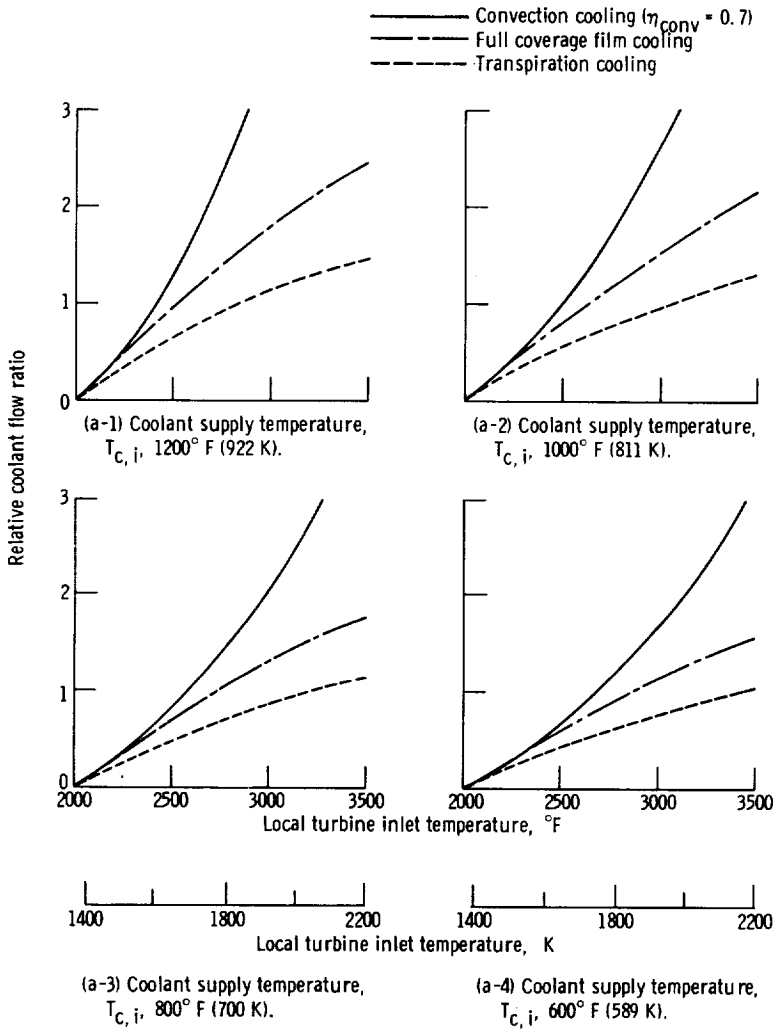

(a) Outside wall temperature for all cooling methods, $T_{B,o}$, 2000° F (1367 K).

Figure 5. - Relative coolant flow requirements for stator vane leading edge. Vane leading edge diameter, D, 0.25 inch (6.35 mm); gas pressure, $p'_{g,s}$, 20 atmospheres (202.6 N/cm^2).

effectiveness η_{conv} of 0.7. The trends in these curves are similar to those for the aft section of the stator vanes and rotor blades shown in figures 3 and 4 except that the cooling improvement with full coverage film and transpiration cooling is less impressive. At least a partial explanation for the smaller difference in coolant flow requirements for the three methods of cooling results from the assumption that a permissible leading edge material temperature is 2000° F (1367 K), whereas the limiting temperature assumed in the aft section of the stator vanes was 1800° F (1255 K). This higher material temperature benefits convection cooling due to the larger temperature difference between the inner wall temperature and the cooling air temperature. The coolant flow requirements for transpiration and full coverage film cooling relative to convection

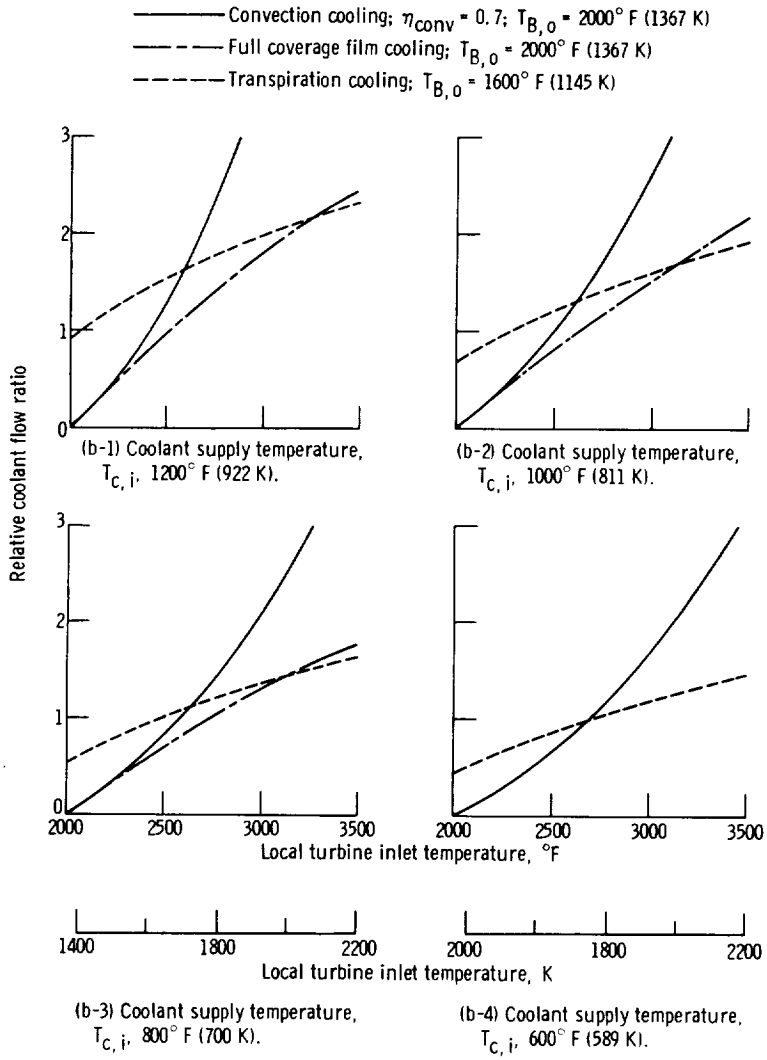

(b) Transpiration cooled vane temperature reduced to 1600° F (1145 K).

Figure 5. - Concluded.

cooling in figure 5(a) at the higher turbine inlet temperatures are similar to those in figures 3 and 4 at lower turbine inlet temperatures. These results occur from the relatively less difficult cooling requirement at the leading edge due to a higher assumed material temperature.

The comparison shown in figure 5(a) is somewhat unrealistic because at the present time a material temperature as high as 2000° F (1367 K) is not possible for transpiration cooling. At such high temperature levels oxidation becomes severe in porous materials and clogging occurs. At the present state-of-the-art, a more realistic permissible porous material temperature is 1600° F (1145 K). Additional discussion of this oxidation problem is given in a later section of the report. Figure 5(b) compares convection full coverage film and transpiration cooling coolant flow requirements for the case where the

material temperature for convection and full coverage film cooling is 2000° F (1367 K) and the material temperature for transpiration cooling is 1600° F (1145 K). With this material temperature limitation on transpiration cooling, it can be seen that the superiority of transpiration cooling relative to convection cooling disappears for gas temperature less than about 2600° F (1700 K). The superiority over full coverage film cooling disappears for gas temperatures less than about 3200° F (2033 K).

Although not shown in figures 3 and 4, similar trends exist for the aft sections of turbine blades and vanes, but the gas temperature levels at which transpiration cooling becomes superior to convection and full coverage film cooling are lower in the aft section of the blades and vanes.

The results shown in figure 5 are for a gas pressure of 20 atmospheres (202.6 N/cm^2). It will be pointed out later that coolant flow requirements are substantially increased for convection cooling as gas pressures are increased, but not for film and transpiration cooling. Therefore, transpiration cooling will show a greater superiority over convection cooling gas pressures in excess of 20 atmospheres (202.6 N/cm^2).

Convection, Film, and Transpiration Heat Transfer

The marked improvement in cooling air requirements for transpiration and film cooling relative to convection cooling can be more easily understood with the help of figure 6. This figure compares the gas to surface heat-transfer coefficients, heat flux (Q/A), and cooling air temperature rise for the three methods of cooling. With convection cooling the gas-to-surface heat-transfer coefficient gradually increases (fig. 6(a)) as turbine inlet temperatures increase due primarily to increased gas thermal conductivity with increasing temperature. With transpiration cooling, however, the heat-transfer coefficient decreases with increasing turbine inlet temperature. This decrease results from steadily increasing coolant flow rates which provide a thicker and thicker insulating layer of air over the cooled surface. The heat-transfer coefficient for full coverage film cooling lies between that for convection and transpiration cooling, but it is not an average of the other two values. For a given turbine inlet temperature and material temperature, the coolant flow requirement is higher for full coverage film cooling than for transpiration cooling. This higher coolant flow causes the film cooling heat-transfer coefficient to be closer to the transpiration coefficient than to the convection coefficient.

The heat fluxes shown in figure 6(b) are exactly as one would expect based on the heat-transfer coefficients since the driving temperature difference between the gas and the surface is identical for all three methods of cooling. The temperature rise plotted in figure 6(c) illustrates the second reason for the superiority of transpiration and film cooling over convection cooling. The solid curves illustrate the temperature difference

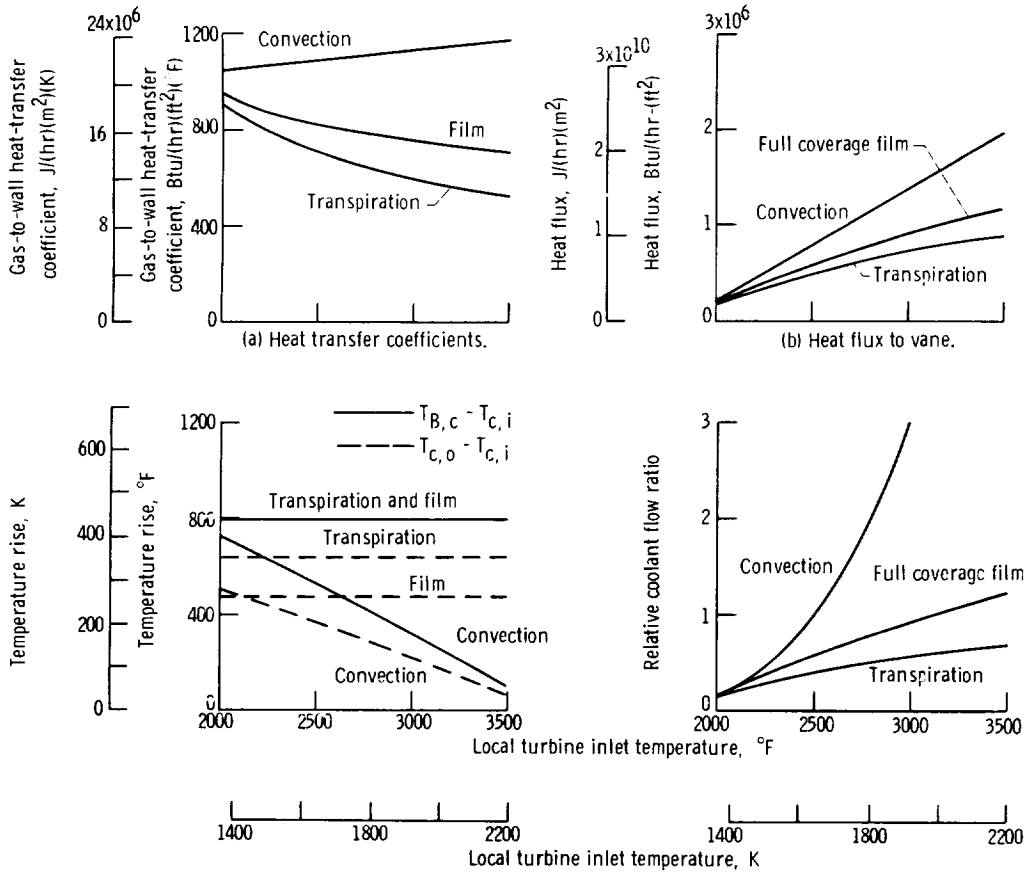

Figure 6. - Comparison of convection, full coverage film, and transpiration cooling heat-transfer effects for aft section of stator vanes. Outside wall temperature, $T_{B,o}$, 1800° F (1255 K); coolant supply temperature, $T_{c,i}$, 1000° F (811 K); thermal effectiveness for convection, η_{conv}, 0.7; thermal effectiveness for film cooling, η_{film}, 0.6; thermal effectiveness for transpiration cooling, η_{trans}, 0.8; wall thickness, t, 0.050 inch (1.27 mm); gas pressure, $p'_{g,s}$, 20 atmospheres (202.6 N/cm²).

between the hottest metal in contact with the coolant ($T_{B,c}$) and the coolant supply temperature ($T_{c,i}$). This temperature difference remains constant as turbine inlet temperature is increased for transpiration and full coverage film cooling since $T_{B,c}$ is the outside wall temperature. For convection cooling, however, the higher heat fluxes at high trubine inlet temperature result in an increasing temperature drop through the wall. Since the temperature difference ($T_{B,c} - T_{c,i}$) on the coolant side of the wall for convection cooling is the difference between the inside wall temperature ($T_{B,c}$ for convection) and the cooling air temperature ($T_{c,i}$), the heat that can be transferred to the cooling air decreases as the turbine inlet temperature increases.

The temperature rise of the cooling air, shown by the dashed lines in figure 6(c), is a direct measure of the heat absorbed per unit of cooling air weight flow rate. This temperature rise is influenced by both the cooling air thermal effectiveness η and the

maximum surface temperature in contact with the cooling air. This temperature rise is constant for transpiration and full coverage film cooling over the entire range of turbine inlet temperatures, but it decreases for convection cooling as turbine inlet temperature is increased. The result of these combined effects is shown in figure 6(d) as a plot of relative coolant flow ratio against turbine inlet temperature.

Factors Affecting Heat Transfer

The comparisons that have been made thus far have been for constant gas pressure, material temperature, wall thickness, and leading edge radius. These factors influence cooling air flow requirements and will be discussed in this section. This discussion will be limited to stator vanes. The trends for rotor blades are similar.

Gas pressure. - Figure 7 shows how gas pressure affects the cooling air requirements per unit surface area for convection, full coverage film, and transpiration cooling for stator vanes. It will be observed that gas pressure (a function of compressor pressure ratio) has a significant effect on coolant flow ratio requirements with convection cooling but no effect with film cooling or transpiration cooling for the assumptions used in this analysis.

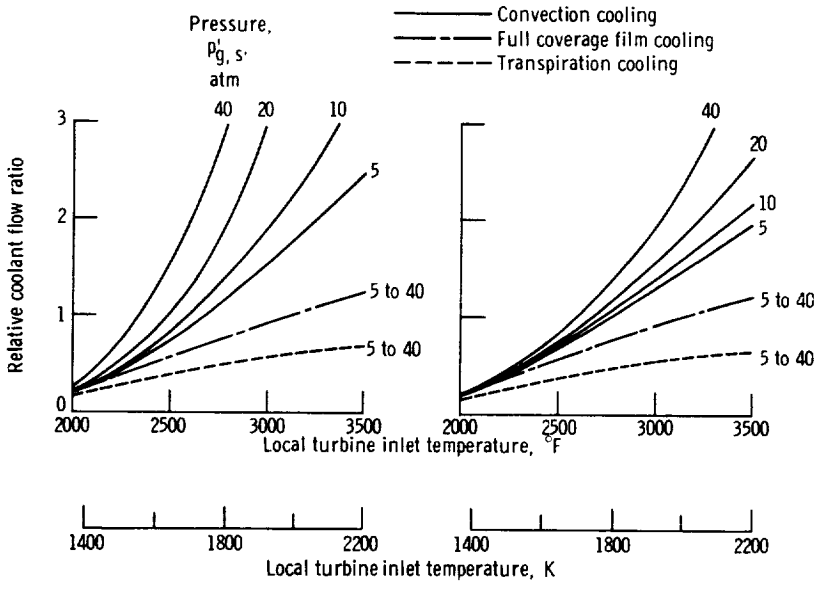

(a) Wall thickness, t, 0.050 inch (1.27 mm).

(b) Wall thickness, t, 0.020 inch (0.51 mm).

Figure 7. - Effect of gas pressure on relative coolant flow ratio requirements for aft sections of stator vanes. Outside wall temperature, $T_{B,o}$, 1800° F (1255 K); coolant supply temperature, $T_{c,i}$, 1000° F (811 K); thermal effectiveness for convection cooling, η_{conv}, 0.7.

Figure 7(a) shows that as gas pressure is increased above 20 atmospheres (202.6 N/cm^2) convection cooling requires excessive cooling air at local turbine inlet temperatures much above 2500° F (1644 K) for the aft section of stator vanes having a thickness of 0.050 inch (1.27 mm). The reason for this rapid rise in cooling airflow with increasing compressor pressure ratio is the high heat flux that results from increased gas-to-surface heat-transfer coefficients at high pressures. These increased heat fluxes cause a large temperature drop through the wall from the conduction process. As a result, the inside wall temperature begins to approach the cooling air temperature for a constant maximum outside wall temperature. This low inside wall temperature can make convection cooling impractical.

With transpiration and full coverage film cooling, the maximum temperature difference between the cooling air and wall temperature remains constant regardless of heat flux (see fig. 6(c)). As a result, compressor pressure ratio does not influence the coolant flow ratio for film and transpiration cooling.

Wall thickness. - Much of the difficulty in convection cooling at high compressor pressure ratios and high temperatures results from the temperature drop through the blade or vane wall. Thinner walls reduce this temperature drop. Figure 7(b) shows coolant flow requirements for a wall thickness of 0.020 inch (0.51 mm) for the aft section of the stator vane. Comparison of figures 7(a) and (b) shows that the thinner wall substantially reduces the coolant flow requirements at high gas temperatures and high gas pressures. Wall thickness has no effect on full coverage film or transpiration coolant flow ratio requirements based on the assumptions of this analysis. As wall thickness is reduced for full coverage film and transpiration cooled blades and vanes, it may be more difficult to obtain high values of cooling air thermal effectiveness η because there will be less surface area in the film cooling holes or in the porous wall for convection heat transfer to heat the cooling air. The results in figure 7 do not account for any change in cooling air thermal effectiveness with wall thickness for any of the three methods of cooling.

Figure 8 shows both cooling air requirements and the temperature drop through the wall thickness for convection cooling for a gas pressure of 40 atmospheres (405.3 N/cm^2) and a range of wall thickness. In the aft section of the stator vane the figure shows that at a turbine inlet temperature of about 2650° F (1728 K) reducing the wall thickness from 0.050 to 0.020 inch (1.27 to 0.508 mm) reduces the cooling airflow requirements by almost a factor of 2.5. This same reduction in wall thickness for a constant coolant flow would permit increasing the allowable local turbine inlet temperature from about 2650° to 3200° F (1728 to 2033 K). The results in figures 7 and 8 show that there is a significantly beneficial effect of reducing blade or wall thickness for engines with high compressor pressure ratios and high turbine inlet temperatures from the standpoint of cooling airflow requirements. It is realized, of course, that structural

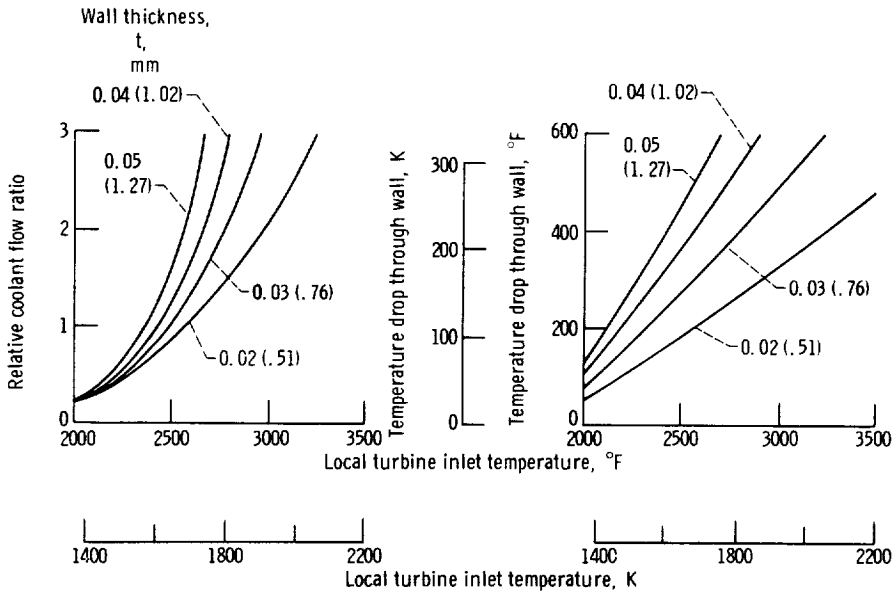

Figure 8. - Effect of convection cooled aft section stator vane wall thickness on relative coolant flow requirements and temperature drop through wall. Outside wall temperature, $T_{B,o}$, 1800° F (1255 K); coolant supply temperature, $T_{c,i}$, 1000° F (811 K); thermal effectiveness, η_{conv}, 0.7; vane wall thermal conductivity, k_B, 12 Btu per hour-foot-°F (20.75 J/(sec)(m)(K); gas pressure, $p'_{g,s}$, 40 atmospheres (405.3 N/cm^2).

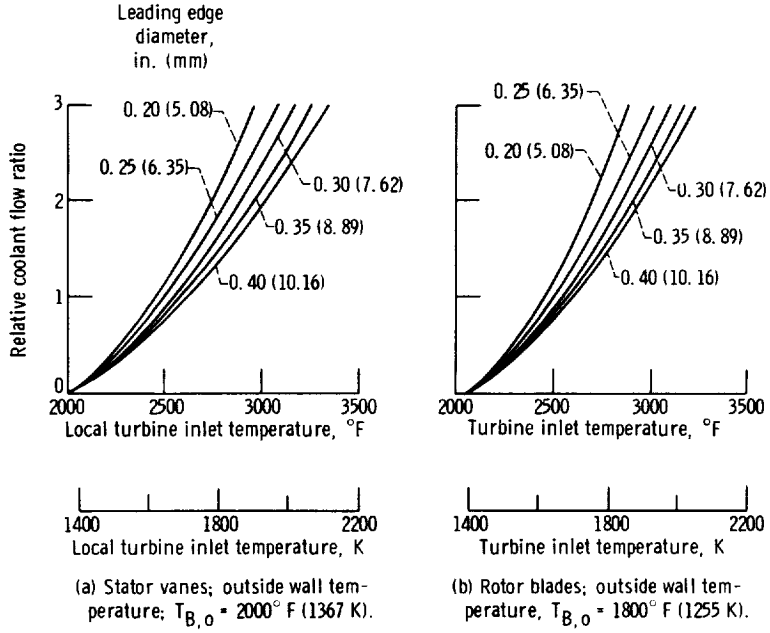

(a) Stator vanes; outside wall temperature; $T_{B,o}$ = 2000° F (1367 K).

(b) Rotor blades; outside wall temperature, $T_{B,o}$ = 1800° F (1255 K).

Figure 9. - Effect of leading edge diameter on relative coolant flow requirements. Coolant supply temperature, $T_{c,i}$, 1000° F (811 K); thermal effectiveness, η_{conv}, 0.7; wall thickness, t, 0.050 inch (1.27 mm); gas pressure, $p'_{g,s}$, 20 atmospheres (202.6 N/cm^2).

considerations such as foreign object damage, gas pressure forces, and oxidation influence the minimum allowable wall thickness.

Leading edge diameter. - As shown in equation (12), the gas-to-wall heat-transfer coefficient in the leading edge is influenced by the leading edge diameter. Increasing this diameter permits lowering the heat-transfer coefficient and the heat flux. Figure 9 shows the beneficial effect of increasing the leading edge diameter for stator vanes and rotor blades for convection cooling. Although not shown, the results are similar for full coverage film and transpiration cooling.

Cooling air temperature. - The effects of cooling air temperature on coolant flow requirements were shown in figures 3 to 5. Figure 10 shows a replot of some of the data from figure 3 in a manner that better illustrates the sensitivity of the three methods of cooling to cooling air temperature. The results for convection cooling are for a thermal effectiveness η_{conv} of 0.7. Figure 10 shows that cooling air temperature has a

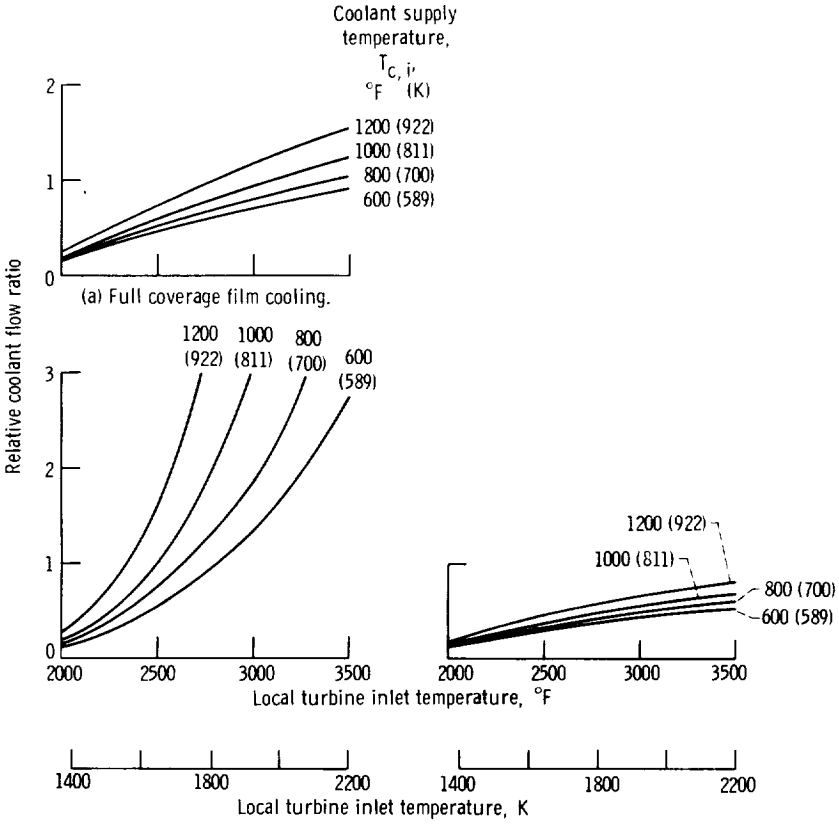

Figure 10. - Effect of cooling air temperature on relative coolant flow requirements for aft section of stator vanes. Outside wall temperature, $T_{B,o}$, 1800° F (1255 K); wall thickness, t, 0.050 inch (1.27 mm); gas pressure, $p_{g,s}$, 20 atmospheres (202.6 N/cm^2).

very marked effect on cooling airflow requirements for convection cooling. It shows that about the only hope for exceeding a turbine inlet temperature of 3000° F (1922 K) with convection cooling with an external wall surface temperature of 1800° F (1255 K) and a wall thickness of 0.050 inch (1.27 mm) without excessive coolant flows is to reduce the cooling air temperature by several hundred degrees below the compressor discharge temperature (which will usually be on the order of 1000° to 1200° F or 811 to 922 K). Such an approach would require rejecting heat from the cooling air to fuel or engine bypass air. With transpiration or full coverage film cooling, however, cooling air temperatures up to 1200° F (922 K) could probably be tolerated. Although it would be beneficial to reduce cooling air temperature from the standpoint of cooling air requirements, the mechanical complexity may not be warranted.

Material temperature. - The effect of material temperature on the cooling airflow requirements for stator vanes is shown in figure 11. The material temperatures shown may not in all cases be feasible for cooled turbines, but the calculations were made to illustrate the benefits that might be obtained through material improvements. The figure

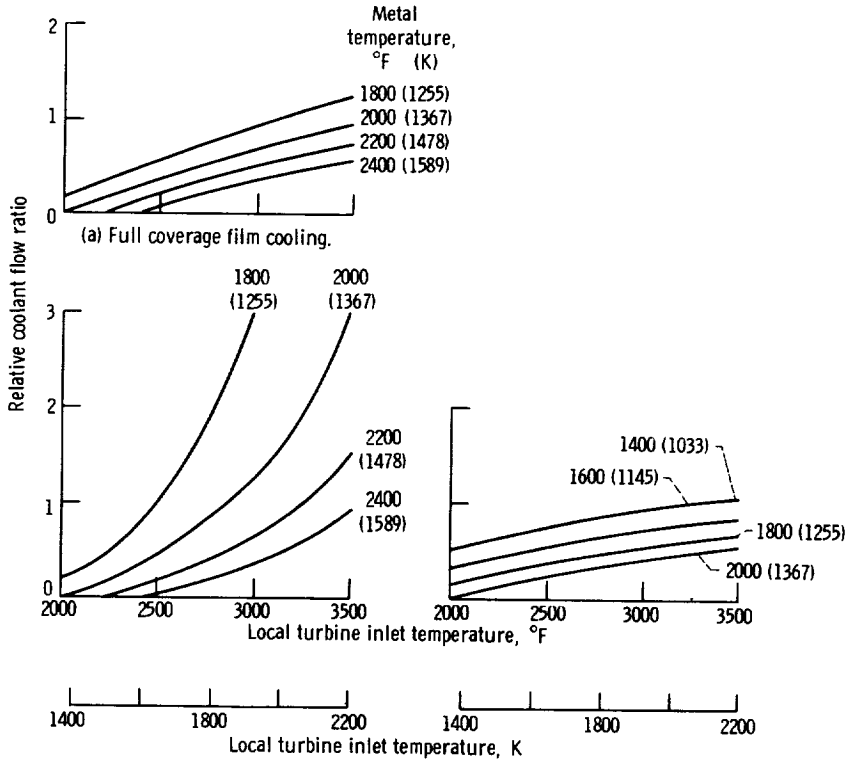

Figure 11. - Effect of stator vane aft section metal temperature on relative coolant flow requirements. Coolant supply temperature, $T_{c,i}$, 1000° F (811 K); wall thickness, t, 0.050 inch (1.27 mm); gas pressure, $p'_{g,s}$, 20 atmospheres (202.6 N/cm^2).

shows that increasing stator vane material temperature to 2200° F (1478 K) makes convection cooling possible up to local turbine inlet temperatures of 3500° F (2200 K) for a gas pressure of 20 atmospheres (202.6 N/cm^2) and wall thicknesses of 0.050 inch (1.27 mm). Although 2200° F (1478 K) is approaching the melting point of nickel base alloys, which are the primary materials in use and under development for turbine blades and vanes, there are indications that some materials can operate for a few hours at this temperature in stator vanes. Transpiration and film cooling show a lower sensitivity to material temperature than convection cooling. Local turbine inlet temperatures up to 3500° F (2200 K) are feasible with considerably lower material temperatures for transpiration and advanced film cooling. In previous figures the material temperature for transpiration cooled stators was considered to be 1800° F (1255 K). With presently available transpiration cooled materials and very long time operation the material temperature may in some cases have to be reduced to as low as 1400° F (1033 K) in order to eliminate oxidation problems. If the material temperature had to be reduced from 1800° to 1400° F (1255 to 1033 K), figure 11 shows that the transpiration cooling coolant flow ratio would have to be almost doubled at a local turbine inlet temperature of 2500° F (1644 K), and it would have to be increased about 50 percent at a local turbine inlet temperature of 3500° F (2200 K). A potential transpiration material with a high temperature capability will be discussed later.

Comparing figure 11(b) with figure 3 shows that improvement in materials to permit higher material temperatures results in a much greater potential for increasing turbine inlet temperature than can be obtained by improving the cooling configuration (increasing η_{conv}) above that for the better existing designs. Increasing material temperature about 100° F (56 K) is approximately equivalent to increasing η_{conv} from 0.7 to 1.0.

By taking partial derivatives of equation (6) for constant h_{conv} we find that

$$\frac{\left(\frac{\partial w_c}{\partial T_{B,o}}\right)}{\left(\frac{\partial w_c}{\partial T_{c,i}}\right)} = -\frac{T'_g - T_{c,i}}{T'_g - T_{B,o}}$$

Since $T_{c,i}$ is always less than $T_{B,o}$ it follows that the reduction in coolant flow from increasing blade or vane metal temperature is larger than that obtained for decreasing cooling air temperature by the same amount. The same result can be observed by inspection of figures 10(b) and 11(b).

Blade Life and Wall Temperature Drop

Turbine blade life is influenced by stress level, temperature level of the blade material, material strength at high temperatures, and thermal stresses that develop as a result of temperature variations in the wall. For high heat fluxes the temperature drop through the wall may become as large or larger than the variations around the blade periphery, therefore, these temperature drops become of considerable importance.

Temperature drop. - The temperature drop through a wall having a thickness of 0.050 inch (1.27 mm) is shown in figure 12 for convection cooling, full coverage film cooling, and transpiration cooling for ranges of turbine inlet temperature and gas pressure. Figure 12(b) shows the temperature drop for convection cooling. For these cal-

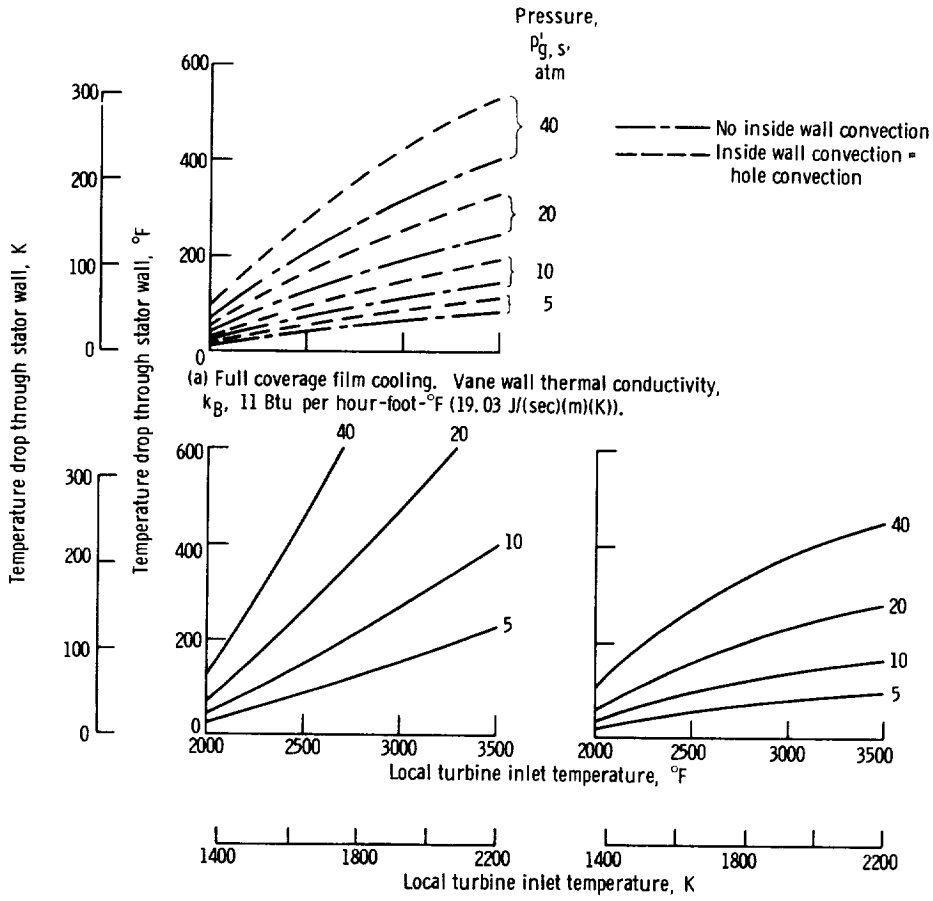

(a) Full coverage film cooling. Vane wall thermal conductivity, k_B, 11 Btu per hour-foot-°F (19.03 J/(sec)(m)(K)).

(b) Convection cooling. Vane wall thermal conductivity, k_B, 12 Btu per hour-foot-°F (20.75 J/(sec)(m)(K)); thermal effectiveness, η_{conv}, 0.7.

(c) Transpiration cooling. Vane wall thermal conductivity, k_B, 8 Btu per hour-foot-°F (13.84 J/(sec)(m)(K)).

Figure 12. - Temperature drop through 0.050 inch (1.27 mm) wall of aft section of stator vanes. Outside wall temperature, $T_{B,o}$, 1800° F (1255 K); coolant supply temperature, $T_{c,i}$, 1000° F (811 K).

culations, the temperature difference between the outside wall surface temperature and the cooling air was 800° F (444 K). When the temperature drop through the convection cooled wall becomes a significant portion of this 800° F (444 K) maximum possible temperature difference, convection cooling becomes very difficult. The very high wall temperature drops in figure 12(b) illustrate this difficulty.

The temperature drops through the wall for full coverage film cooling (fig. 12(a)) are smaller than those for convection cooling. Temperature drops for two modes of transferring the heat with film cooling are shown. The long dash - short dash lines labeled "no inside wall convection" assume that the entire temperature rise of the coolant takes place within the wall in a manner somewhat similar to transpiration cooling. In order for heat transfer to occur in this manner, a large heat-transfer surface is required within the wall as could possibly be obtained by having sharply slanted passages similar to those shown in figure 1(c). In some cases, however, shorter passages may be desired from the standpoint of fabrication and structural considerations. For such cases internal convection cooling would be required in conjunction with the film cooling in order to effectively use a significant portion of the potential temperature rise of the cooling air ($T_{B,o} - T_{c,i}$). The dashed curves in figure 12(a) illustrate the case where convection on the inside wall provides half of the temperature rise of the cooling air and the other half occurs due to convection within the film cooling holes. This mode of heat transfer results in higher temperature drops throughout the wall than for the case where all of the heat transfer to the cooling air occurs inside the film cooling passages; however, these wall temperatures drops are still significantly lower than those occurring with convection cooling.

The temperature drops through the wall for transpiration cooling (fig. 12(c)) are just slightly higher than those for full coverage film cooling where there is no inside wall surface convection. The difference between these temperature drops results from transpiration cooling materials having a lower effective thermal conductivity than full coverage film cooling. The calculations in figure 12(c) are based on a thermal conductivity of 8 Btu per hour-foot-°F (13.84 J/(sec)(m)(K)) which corresponds to a porosity of the material of about 15 percent (ref. 11). If the thermal conductivity were lower, the temperature drops would be higher. Calculations made for a very low thermal conductivity of 1.5 Btu per hour-foot-°F (2.59 J/(sec)(m)(K)) for a gas pressure of 40 atmospheres (405.3 N/cm^2) showed the temperature drop through the wall approaching 800° F (444 K), the maximum possible, since this is the temperature difference between the outside wall temperature and the cooling air supply temperature.

Figure 12 shows the highest temperature drops for convection cooling, and those for transpiration and full coverage film cooling temperature drops are close to each other. Consequently, if stress concentrations from film cooling passages are neglected, thermal stress from through the wall temperature drops will be smaller for full coverage

film cooling than for convection cooling. Since the structure for transpiration cooling is not homogeneous, it is difficult to evaluate how the thermal stress for transpiration cooling will compare with convection and full coverage film cooling.

The temperature drops through blade and vane walls can be reduced by decreasing the wall thickness. Figure 13 shows wall temperature drops for a wall thickness of 0.02 inch (0.51 mm) as opposed to the 0.05 inch (1.27 mm) wall thickness of figure 12. In the calculations of this report, blade wall thermal conductivity was assumed invariant with temperature. As a result, the temperature drop through the stator wall for convection cooling in figure 13(b) are exactly two-fifths of the temperature drop shown in figure 12(b). These lower temperature drops significantly improve the convection cooling capabilities as previously discussed in connection with figure 8. The temperature drop through the wall for full coverage film and transpiration cooling (fig. 13(a) and (c)) are reduced by approximately the same percentage as for convection cooling when wall thickness is reduced. In the calculations of this report the thinner walls for film and trans-

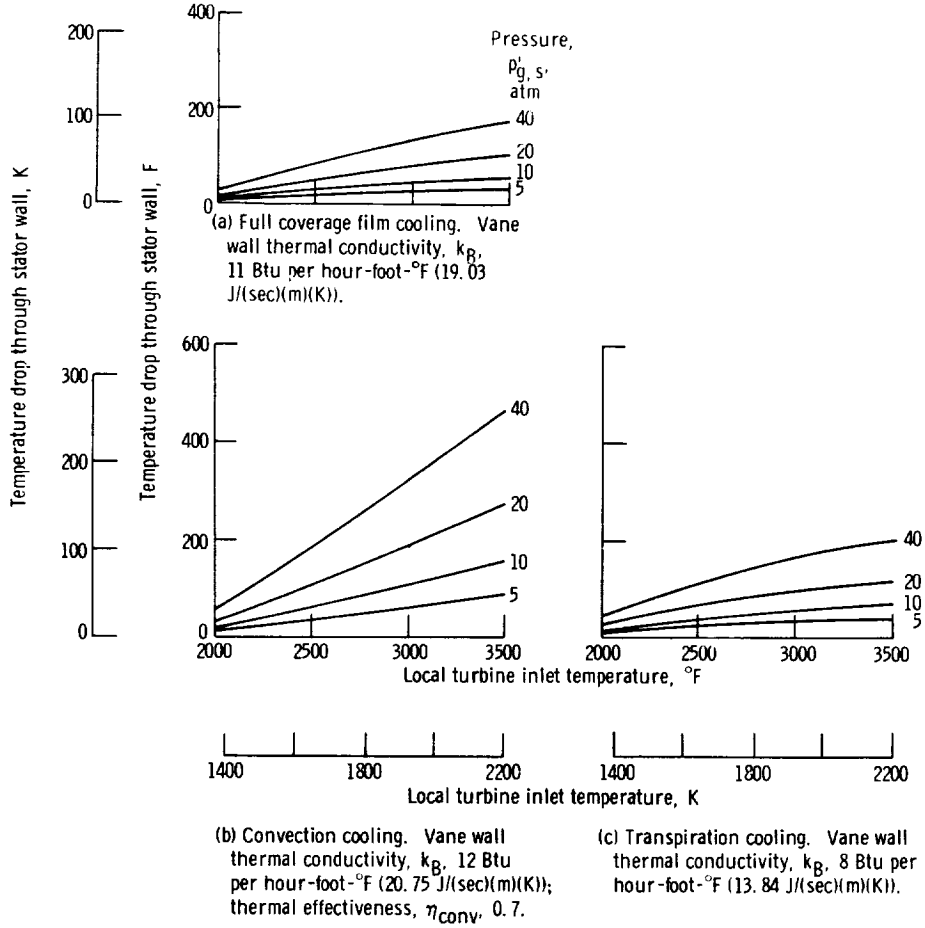

Figure 13. - Temperature drop through 0.020 inch (0.51 mm) wall of aft section of stator vanes. Outside wall temperature, $T_{B,o}$, 1800° F (1255 K); coolant supply temperature, $T_{c,i}$, 1000° F (811 K).

piration cooling had no effect on coolant flow requirements because η_{film} and η_{trans} were assumed to be independent of wall thickness. In actual practice, however, the cooling air thermal effectiveness may decrease as wall thickness decreases. The trends for full coverage film and transpiration cooling would then be opposite to those for convection cooling. Convection cooling will require less cooling air with thinner walls, while the other two methods may require slightly more cooling air.

Blade life. - The results of the blade life analyses for an outer surface temperature of 1800° F (1255 K) and wall temperature drops of 48°, 300°, 480°, and 600° F (27, 167, 267, and 333 K) at centrifugal stress levels of 26 000 and 39 000 pounds per square inch (179 and 269 N/mm^2) are presented in table II. Results under conditions of steady-state creep damage are presented in the fifth and sixth columns, fatigue damage in the seventh and eighth columns, and combined creep and fatigue damage without and with holes in the ninth and tenth columns. In addition, for the last condition the temperatures and total stresses after relaxation at the critical nodes, or nodes with the worst combination of stress and temperature, are shown in the third and fourth columns. In general, the critical nodes were near the inside surface of the airfoil shell in the trailing edge region.

An exhaustive discussion of the results in table II would be complicated and lengthy because of the frequent changes in critical locations. It is not the purpose of this study to perform rigorous analyses of blade lives and the actual life values are not important. The trends are important; therefore, the discussion of table II is limited to illustrating general trends and effects.

TABLE II. - RESULTS OF BLADE LIFE ANALYSES

[Outer surface temperature, 1800° F (1255 K).]

Wall temperature drop, °F (K)	Centrifugal stress, ksi (N/mm^2)	Critical node[a]		Steady-state life		Fatigue life for 2-hour cycles		Combined life based on life-fraction rule	
		Total stress, ksi (N/mm^2)	Temperature, °F (K)	Based on initial condition, hr	Based on stress relaxation, hr	Without holes, hr	With holes, hr	Without holes, hr	With holes, hr
48 (27)	26 (179)	27.8 (192)	1762 (1234)	48	117	(b)	(b)	117	117
300 (167)	↓	46.2 (319)	1513 (1096)	72	2357	↓	28 000	2357	2328
480 (267)	↓	89.5 (617)	1340 (1000)	157	462	↓	4 800	462	421
600 (333)	↓	93.0 (641)	1275 (964)	702	1929	↓	2 500	1929	1341
48 (27)	39 (269)	41.3 (285)	1762 (1234)	7	12	↓	(b)	12	12
300 (167)	↓	53.1 (366)	1538 (1110)	8	231	↓	8 000	231	228
480 (267)	↓	101.8 (702)	1340 (1000)	76	83	↓	2 100	76	80
600 (333)	↓	105.1 (725)	1225 (936)	125	575	↓	1 200	575	399

[a]For combined life with holes.

[b]Not fatigue limited within 30 000 hr.

The main conclusion to be drawn from table II is that increasing the wall temperature drop does not necessarily shorten the blade life. Actually, the shortest blade lives occurred with the smallest wall temperature drop. As expected, the thermal stresses (difference between total and centrifugal stress in table II) increased while the temperature levels decreased at the critical nodes with increasing wall temperature differences.

The improved material properties at the lower node temperatures have a greater effect in increasing the steady-state lives at the initial conditions (fifth column) than the accompanying rise in thermal stresses have in shortening life. However, when stress relaxation was taken into account the results did not show such a simple trend because of the complexity of the relaxation effects. This relaxation tends to proceed rapidly when thermal stresses and temperatures are high and slowly when they are low. The erratic nature of the results shown in the sixth column arises from two factors: (1) as the wall temperature drop increases, the relaxation shifts from the critical nodes near the cooler inside surface to the hotter nodes with high compressive stresses near the outer surface, and (2) the counteracting relaxirg effects from increasing thermal stresses with decreasing temperature levels at the critical nodes.

The low steady-state lives with the 48° F (27 K) wall temperature drop were caused by the high bulk metal temperature. When the wall temperature drop was increased to 300° F (167 K), the blade life was also increased because of the reduction in the bulk metal and critical node temperatures. At this condition the compressive thermal stresses near the outside surface were minor. Therefore, there was a large relaxation in the tensile thermal stresses which resulted in about a thirtyfold improvement in life over the initial conditions. When the wall temperature difference reached 480° F (267 K) the compressive stresses became predominate and the relaxation effects caused these stresses to be relieved with very little relaxation of the tensile stresses. As a result, stress relaxation did not appreciably improve blade life with a 480° F (267 K) temperature drop through the wall because failure results from tension rather than compression. A 600° F (333 K) wall temperature drop resulted in somewhat higher compressive stresses and strains and an even greater shift of the relaxation process to the vicinity of the hot outer wall. However, the further reduction in the critical node temperature and the resulting material properties improvement caused the steady-state life to increase over that for the 480° F (267 K) temperature drop.

The fatigue life decreased with increasing wall temperature drop because of the greater total strain levels which are the predominating influence on fatigue. The effect of strain cycling on life for IN 100 materials is relatively insensitive to temperature level as indicated in reference 18 for test temperatures from 1000° to 2000° F (811 to 1367 K). However, none of the total strain levels computed for the cases which were considered were sufficiently high to cause fatigue failure within 30 000 hours at nodes where there were no holes present.

The deleterious effect of holes on the combined cyclic and steady-state lives nullifies some of the heat-transfer advantages of film and transpiration cooling over convection cooling.

Turbine Materials

In previous discussions in this report, material temperatures have been assumed with little justification given for the choice of values. The majority of the calculations were made at conservative temperature values for the present state of the art. Calculations were also made to indicate how coolant flow requirements would vary if the required material temperatures were increased or decreased.

Blade and vane materials. - Figure 14 illustrates the present and expected future temperature limitations for several classes of rotor blade and stator vane materials. At the present time, rotor blades are made exclusively of superalloys (nickel or cobalt base). Strength capabilities of the best of these superalloys limit their use temperature to slightly over 1800° F (1255 K) for rotor blades. Oxidation begins at lower temperatures (about 1700° F or 1200 K). As a result oxidation-corrosion protective coatings are required when long-life is required. Based on research at NASA and other organizations, it is expected that the use temperature of superalloys for rotor blades can be extended to about 1900° F (1310 K) within the next few years.

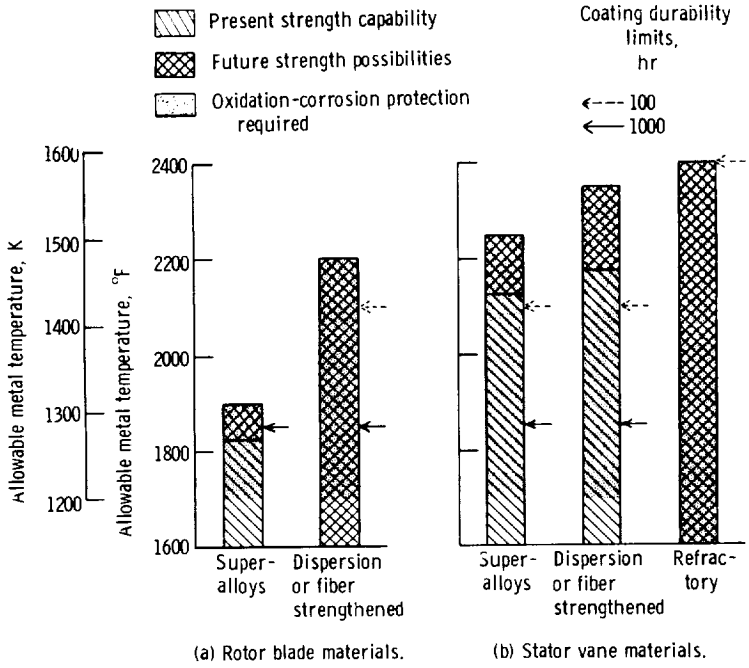

(a) Rotor blade materials. (b) Stator vane materials.

Figure 14. - Turbine material temperature capabilities.

At the present time dispersion and fiber strengthened materials have not found use in turbine rotor blades. Although TD-Ni and TD-NiCr (materials containing a thoria dispersoid) have been successful in increasing the use temperature for low stress applications, their stress carrying capabilities have been too low to use in rotor blades. Research on adding inert dispersoids or refractory fibers to superalloys has given indication that within the next few years such materials might find use in turbine rotor blades with metal temperatures up to 2200° F (1478 K). These materials will still require some form of surface protection from oxidation and corrosion for temperatures above 1700° F (1200 K). This surface protection may determine the maximum operating temperature as shown by the "coating durability limits" in figure 14.

At the present time two classes of the newer materials have the strength to be used in stator vanes at material temperatures above 2100° F (1422 K). These materials include superalloys and the dispersion-strengthened nickel and nickel-chromium alloys, TD-Ni and TD-NiCr. The life of coatings, used to protect stator vane alloys from oxidation, limits the upper use temperature, particularly for long time operation. Within the next few years it is expected that the use temperature of the superalloys can be increased to about 2250° F (1506 K) and the dispersion or fiber strengthened superalloys to about 2300° F (1532 K). It is unlikely that the use temperature can be increased very much higher because the melting point of some of the alloy constituents is being approached. To go to higher material operating temperatures will necessitate switching to refractory alloys. Stator vane material temperatures up to approximately 2400° F (1589 K) may be possible using the refractory columbium alloys. All refractory materials are extremely prone to oxidation; therefore, durable oxidation resistant coatings will be required. It is expected, therefore, that refractory alloys will be used only in applications that do not require long life because coating failure from foreign object damage could cause a rapid oxidation failure of a refractory alloy.

Transpiration and film cooling material oxidation. - Photographs of typical transpiration cooling and full coverage film cooling materials are shown in figure 15. In these materials, the coolant flow passages are small. Oxide films can block these passages and reduce the coolant flow. This blockage causes the material to become hotter due to poorer cooling, and further oxidation is accelerated. As a result, transpiration and full coverage film cooling are much more sensitive to oxidation than convection cooling. NASA research is being conducted on these oxidation problems.

Figure 16 compares the effects of oxidation on the coolant flow rate through transpiration and full coverage film cooling materials. Conventional wire-form transpiration cooling material, such as illustrated in figure 15(a), is compared in figure 16 for two alloys for a range of exposure times at 1800° F (1255 K). Alloy A is a conventional nickel-base alloy (Hastelloy X) commercially used in high temperature applications. At 1800° F (1255 K) oxidation is severe and wire-form transpiration cooling material becomes blocked in less than 400 hours of exposure time. Experimental tests on Alloy B

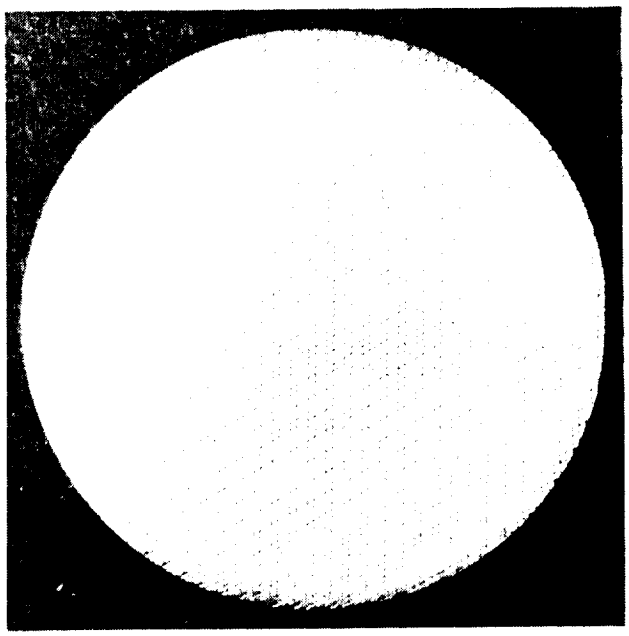

(a) Wire form transpiration cooling material.

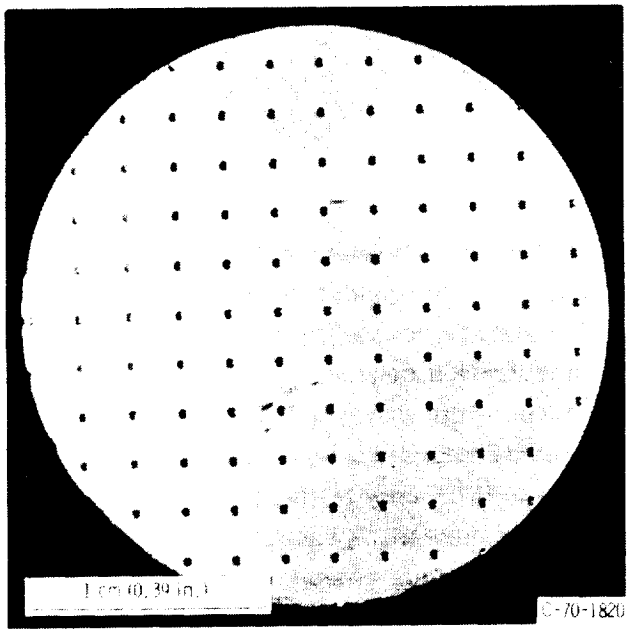

(b) Full coverage film cooling material.

Figure 15. - Surfaces of transpiration and film cooling materials.

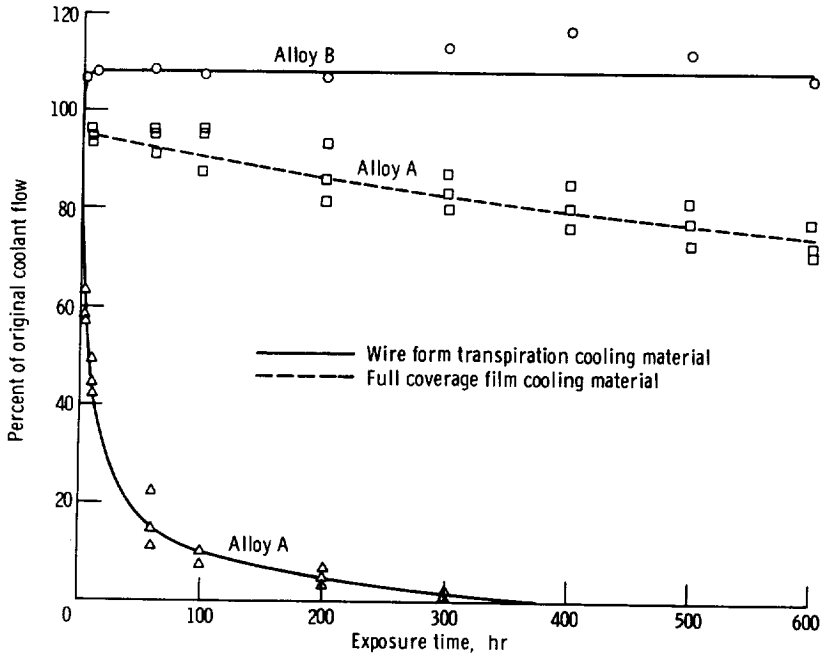

Figure 16. - Coolant flow reduction from oxidation of transpiration and film cooling materials at 1800° F (1255 K). Alloy A, 22Cr-18.5Fe-9Mo-1.5Co-Ni (Hastelloy X); alloy B, 15 Cr-4Al-1Y-Fe (GE 1541).

an iron-chromium-aluminum-yttrium heating element alloy (GE 1541), show some data scatter, but do not indicate any blockage from oxidation after exposures up to 600 hours at 1800° F (1255 K). Research is continuing on methods for best fabricating this material into a wire-form transpiration cooling material.

Figure 16 also compares a full coverage film cooling material with the wire-form transpiration cooling material when both materials are made from the nickel-base alloy A (Hastelloy X). These two material forms initially had the same coolant flow rate per unit surface area for the same pressure drop across the material surface. Because of the larger, but fewer coolant passages in the full coverage film cooling material, its clogging tendency due to oxidation was greatly reduced compared to the wire-form transpiration cooling material.

The results of these investigations indicate that transpiration cooling materials can probably be operated at material temperatures on the order of 1800° F (1255 K) within the near future. Even higher temperatures may be possible for full coverage film cooling materials. It may be possible to provide oxidation resistant coatings inside the film cooling holes to further reduce blockage by oxides.

Factors Not Considered in Analysis

This analysis considered only the cooling airflow requirements for first-stage turbine stator and rotor vanes and blades. It did not consider the problems of shroud cooling, nor the aerodynamic effects of the discharge of the cooling air into the gas stream.

Considering only the first stage of the turbine can be defended on the basis that cooling is most difficult for this stage due to the high temperature levels at this location. The results presented can also be used as an approximation for the second stage of the turbine if the turbine inlet temperatures are considered as temperatures at the inlet of the second stage.

An analysis was not made on the cooling requirements for the turbine shroud. Shroud cooling will become a very important requirement at high turbine inlet temperatures, and it must be considered. The general trends shown in this report for blade and vane cooling should provide at least an indication of the relative merits of the three general air cooling schemes as applied to shroud cooling.

The aerodynamic effects of cooling air discharge on the turbine performance constitute a subject of too large a scope to include in this report. In any cooled turbine design, however, the cooling air flow must be considered in the aerodynamic design. The cooling air flow effects naturally become larger and more important at the higher flow rates that will be experienced at very high turbine inlet temperatures. In general, it can probably be concluded that for equal discharge of cooling air, convection cooled turbines will have superior aerodynamic performance than film or transpiration cooled turbines. The discharge of film or transpiration cooling air into the vane or blade boundary layer usually has deleterious effects on turbine performance, particularly if its effect was not considered properly in the aerodynamic design. The results of this present investigation, however, indicate that to achieve the very high turbine inlet temperatures and corrected compressor pressure ratios that are expected for future engines, transpiration and/or full coverage film cooling may be required. More research will be needed to evaluate the aerodynamic effects of transpiration and film cooling on turbine aerodynamic performance.

SUMMARY OF RESULTS

The results of this investigation can be summarized as follows:

1. Convection cooling of turbine blades and vanes becomes very difficult under the combination of high gas temperatures and pressures expected in future engines. High temperature drops through the blade or vane wall reduce the temperature difference between the inside wall surface and the cooling air and correspondingly reduce cooling effectiveness. Reducing wall thickness, developing materials with a higher temperature

capability, or reducing cooling air temperature with heat exchangers will permit operation at higher gas temperatures and pressures, or reduce coolant flow requirements.

2. Reducing wall thickness from 0.050 to 0.020 inch (1.27 to 0.51 mm) could increase permissible turbine inlet temperature by as much as 500° F (278 K) for convection cooling.

3. Local turbine inlet temperatures up to 3500° F (2200 K) are possible for convection cooled stators if a material with a temperature capability of 2200° F (1478 K) can be used.

4. Reducing cooling air temperature from 1000° F (811 K) to 600° F (589 K) could permit increasing turbine inlet temperature as much as 500° F (278 K) for convection cooling.

5. Increasing allowable metal temperatures 100° F (56 K) or reducing cooling air temperature 200° F (111 K) can do more to improve the cooling capabilities of convection cooled blades and vanes than is possible by further improvements in the better convection cooling designs now available.

6. The coolant flow requirements for full coverage film and transpiration cooling are very much lower than for convection cooling at high turbine inlet temperatures and high compressor pressure ratios. These cooling methods can often permit turbine inlet temperatures 1000° F (556 K) higher than permitted with convection cooling at the same coolant flow rates. Cooling air temperature and maximum allowable wall temperature have considerably less effect on the coolant flow requirements for transpiration and full coverage film cooling than for convection cooling.

7. Unless oxidation problems can be overcome in transpiration cooled materials to permit them to operate at temperatures approaching that possible with conventional turbine materials, transpiration cooling may not show advantages over full coverage film cooling except for extremely difficult cooling problems such as local turbine inlet temperatures in excess of about 3200° F (2033 K) at compressor ratios in excess of 20.

8. For a given maximum outside wall temperature (such as an oxidation temperature limit), high temperature drops through the wall thickness are not necessarily detrimental to blade life. Due to the lower average wall temperature with the high temperature drops, such blades or vanes may have longer life than the ones with lower temperature drops.

9. Recent research on both solid and porous turbine blade and vane materials show promise of increasing the permissible material temperatures for convection, film, and transpiration cooled turbine blades and vanes.

Lewis Research Center,
National Aeronautics and Space Administration,
Cleveland, Ohio, June 9, 1970,
720-03.

APPENDIX A

SYMBOLS

A	external blade surface area
A_f	coolant passage flow area
A_i	coolant passage surface area
B	defined by eq. (18)
c_p	specific heat at constant pressure
D	blade or vane leading edge diameter
d	coolant passage height
g	gravitational constant
h	gas-to-surface heat transfer coefficient
h_c	surface-to-coolant heat transfer coefficient
k	thermal conductivity
L	Reynolds number characteristic length (average blade or vane surface distance from leading edge)
M	Mach number
Pr	Prandtl number, $c_p\mu/k$
p	pressure
Q	heat transfer per unit time
R	gas constant
Re	Reynolds number, $\rho VL/\mu$ or $\rho VD/\mu$
St	Stanton number, $h/\rho Vc_p$
T	temperature
T^*	dimensionless wall temperature
t	vane or blade wall thickness
V	velocity
w	coolant flow rate
x	coordinate through vane or blade wall
γ	ratio of specific heats
ζ	fractional portion of total heat transfer to coolant occurring on inside wall surface
η	cooling air thermal effectiveness defined by eqs. (1) and (2)
Λ	recovery factor
μ	viscosity
ξ	x/t
ρ	density
φ	angle measured from stagnation point, deg

Subscripts:

avg	average
B	blade or vane wall
B, c	wall in contact with coolant
c	coolant
conv	convection cooling
e	effective or adiabatic
film	film cooling
g	gas

i	inside of blade or vane (coolant side), or inside surface
o	outside of blade or vane (gas side), or outside surface
ref	reference
s	at stator inlet
trans	transpiration cooling

Superscripts:

'	relative total
$\bar{}$	average over dimension L

APPENDIX B

FILM AND TRANSPIRATION COOLED WALL TEMPERATURE PROFILES

Analysis

A porous wall model shown in figure 17 was used to describe the temperature profiles through the vane or blade wall for both transpiration and film cooling. It was assumed that the porous wall model could be used for the full coverage film cooling case due to the large number of closely spaced holes present.

The heat transfer process was modeled by considering a one-dimensional counterflow situation where heat flowing by conduction through the wall in the negative x-direction is continuously transferred to the coolant in counterflow by convection.

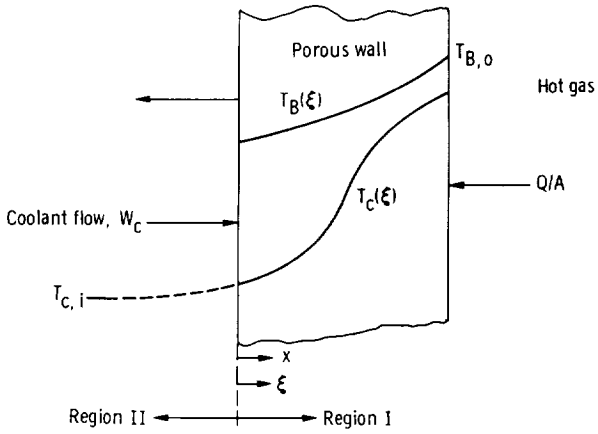

Figure 17. - Porous wall temperature profile model.

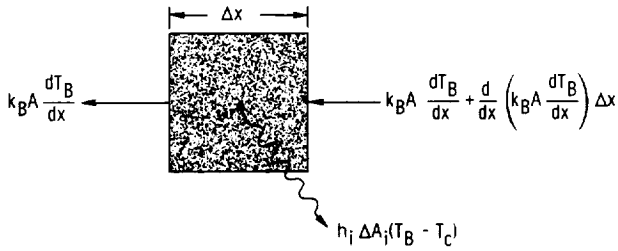

Figure 18. - Typical element of porous wall.

Describing the porous wall as being composed of cooling passages within the matrix material, it was further assumed that conduction in the fluid in region I is negligible compared to that of the matrix.

Consider an element in the porous wall of area A normal to the x-direction as shown in figure 18. An energy balance on this element gives

$$k_B \frac{d^2 T_B}{dx^2} = h_i \frac{\Delta A_i}{A\,\Delta x} (T_B - T_c) \tag{B1}$$

where h_i is the internal matrix surface-to-coolant heat transfer coefficient and ΔA_i is the internal surface area within the element. Defining σ as an internal area density equal to

$$\frac{\Delta A_i}{A\,\Delta x} = \frac{\text{internal surface area}}{\text{volume}}$$

leads to the following expression for the coolant temperature in region I:

$$T_c = T_B - \frac{k_B}{h_i \sigma} \frac{d^2 T_B}{dx^2} \tag{B2}$$

For a homogeneous pore structure, σ is constant with x.

An energy balance on the coolant within the element in figure 18 results in

$$\frac{k_B A}{w_c c_{p,c}} \frac{d^2 T_B}{dx^2} = \frac{dT_c}{dx} \tag{B3}$$

Differentiating equation (B2) with respect to x and substituting into equation (B3) leads to the following equation for the temperature distribution in the matrix material:

$$\frac{d^3 T_B}{dx^3} + \frac{h_i \sigma A}{w_c c_{p,c}} \frac{d^2 T_B}{dx^2} - \frac{h_i \sigma}{k_B} \frac{dT_B}{dx} = 0 \tag{B4}$$

In dimensionless form equations (B2) and (B4) become

$$T_c^* = T_B^* - \frac{1}{\lambda} \frac{d^2 T_B^*}{d\xi^2} \tag{B5}$$

$$\frac{d^3 T_B^*}{d\xi^3} + \beta \frac{d^2 T_B^*}{d\xi^2} - \lambda \frac{dT_B^*}{d\xi} = 0 \tag{B6}$$

where

$$T_B^* = \frac{T_B - T_{c,i}}{T_{B,o} - T_{c,i}}$$

$$T_c^* = \frac{T_c - T_{c,i}}{T_{B,o} - T_{c,i}}$$

$$\xi = \frac{x}{t}$$

$$\lambda = \frac{h_i \sigma t^2}{k_B}$$

$$\beta = \frac{h_i \sigma t A}{w_c c_{p,c}}$$

The solution to equations (B5) and (B6) results in the following expressions for the coolant and wall temperature profiles:

$$T_B^*(\xi) = C_1 + C_2 e^{a_1 \xi} + C_3 e^{a_2 \xi} \tag{B7}$$

$$T_c^*(\xi) = C_1 + C_2 \left(1 - \frac{a_1^2}{\lambda}\right) e^{a_1 \xi} + C_3 \left(1 - \frac{a_2^2}{\lambda}\right) e^{a_2 \xi} \tag{B8}$$

where

$$a_1 = -\frac{1}{2}\left(\beta + \sqrt{\beta^2 + 4\lambda}\right)$$

$$a_2 = -\frac{1}{2}\left(\beta - \sqrt{\beta^2 + 4\lambda}\right)$$

Boundary Conditions

A number of investigators (refs. 21 to 24) have considered various boundary conditions for the porous wall heat-transfer model. None of these were entirely appropriate for the present analysis.

Three boundary conditions are sufficient to evaluate the three constants C_1, C_2, and C_3. The temperature distributions $T_B^*(\xi)$ and $T_c^*(\xi)$ would then be known if the product of the inside surface-to-coolant heat transfer coefficient h_i and the internal

area density σ was known. However, in general, H (where $H = h_i\sigma$) is difficult to determine; hence, a fourth boundary condition was introduced so that the temperature profiles could be determined without explicitly specifying H. The four boundary conditions are

$$T_B^*(1) = 1 \tag{B9}$$

$$T_c^*(1) = \eta \tag{B10}$$

$$\frac{dT_B(0)}{d\xi} = \zeta\eta\frac{\lambda}{\beta} \tag{B11}$$

$$T_c^*(0) = \frac{\beta}{\lambda}\frac{dT_B^*(0)}{d\xi} \tag{B12}$$

The quantity ζ is the fractional portion of heat transferred to the coolant from the inside (x = 0) wall and will be discussed later. The thermal effectivensss η is for either transpiration or film cooling.

The first boundary condition (eq. (B9)) is that of a specified outside wall temperature - 1800° F (1255 K). The boundary condition of equation (B10) is that of a specified cooling effectiveness for either transpiration or film cooling (0.6 for film cooling and 0.8 for transpiration cooling). The boundary conditions at x = 0 for the coolant and the matrix material (eqs. (B11) and (B12)) provide for the possibility of including convection from the inside wall to the coolant. These two conditions are now discussed. From a heat balance on the coolant region II,

$$\frac{Q_2}{A} = k_B\frac{dT_B}{dx}\bigg|_{x=0} = \frac{w_c c_{p,c}}{A}\left[T_c(0) - T_{c,i}\right]$$

or in dimensionless form,

$$\frac{dT_B^*(0)}{d\xi} = \frac{\lambda}{\beta}T_c^*(0)$$

Representing the heat flux Q_2/A as some percentage ζ of the total heat flux to the wall from the hot gas stream (given by eq. (3)) gives

$$\frac{dT_B^*(0)}{d\xi} = \zeta\frac{dT_B^*(1)}{d\xi}$$

and substituting $dT_B^*(1)/d\xi$ from equation (B7) gives

$$\frac{dT_B^*(0)}{d\xi} = \zeta\eta\frac{\lambda}{\beta}$$

A discussion of the choice of ζ values for transpiration and film cooling follows.

It was assumed that conduction in the coolant upstream of $x = 0$ is negligible. This assumption can be justified in the following manner. Consider flow between a series of parallel plates of negligible thickness all at the same temperature at a given x location. If $x = 0$ is the leading edge of the plates, there is no surface area normal to the direction of flow at $x = 0$ from which convection to the upstream coolant can take place - a situation closely approximated by the transpiration cooling case due to the essentially "infinite" number of pores. Results in reference 25 indicate that if $RePr > 50$ (Re based on the hydraulic diameter) conduction in the negative x-direction in the region $x < 0$ is negligible; hence, the approaching fluid does not feel the effects of the plates until it reaches $x = 0$.

In the porous wall case, the Peclet number (RePr) was greater than 100 for typical film cooling hole diameters and transpiration pore sizes at the lowest coolant flow rate. As a result, ζ was set equal to zero for transpiration cooling. Two cases were considered for film cooling, ζ equal to 0 and 0.5. The latter case represents a condition where half the total temperature rise of the coolant takes place upstream of the wall due to convection from the surface in the $x = 0$ plane between the holes.

Solution

The constants C_1, C_2, and C_3 of equations (B7) and (B8) are given

$$C_1 = 0$$

$$C_2 = \frac{\left(a_2 - \frac{\lambda}{\beta}\eta\right)}{(a_2 - a_1)e^{a_1}}$$

$$C_3 = -\frac{\left(a_1 - \frac{\lambda}{\beta}\eta\right)}{(a_2 - a_1)e^{a_2}}$$

With α and ψ defined as

$$\alpha = \frac{\beta}{H}$$

$$\psi = \frac{\lambda}{H}$$

the value of H which satisfies the following equation (from eq. (B11)) was determined numerically:

$$(2 - \eta)\sinh\frac{1}{2}\alpha H\sqrt{1 + \frac{4\psi}{H\alpha^2}} - \eta\sqrt{1 + \frac{4\psi}{H\alpha^2}}\cosh\frac{1}{2}\alpha H\sqrt{1 + \frac{4\psi}{H\alpha^2}} = -\zeta\eta\sqrt{1 + \frac{4\psi}{H\alpha^2}}\, e^{-\frac{1}{2}\alpha H}$$

REFERENCES

1. Stepka, Francis S.: Considerations of Turbine Cooling Systems for Mach 3 Flight. NASA TN D-4491, 1968.

2. Goldstein, R. J.; Eckert, E. R. G.; and Ramsey, J. W.: Film Cooling with Injection Through a Circular Hole. Rep. HTL-TR-82. Minnesota Univ. (NASA CR-54604), May 14, 1968.

3. Metzger, D. E.; Carper, H. J.; and Swank, L. R.: Heat Transfer with Film Cooling Near Nontangential Injection Slots. J. Eng. Power, vol. 90, no. 2, April 1968.

4. Metzger, D. E.; and Fletcher, D. D.: Surface Heat Transfer Immediately Downstream of Flush, Non-Tangential Injection Holes and Slots. Paper 69-523, AIAA, June 1969.

5. Goldstein, R. J.; Eckert, E. R. G.; Eriksen, V. L.; and Ramsey, J. W.: Film Cooling Following Injection Through Inclined Circular Tube. Rep. HTL-TR-91, Minnesota Univ. (NASA CR-72612), Nov. 1969.

6. Moffat, R. J.; and Kays, W. M.: The Turbulent Boundary Layer on a Porous Plate: Experimental Heat Transfer with Uniform Blowing and Suction. Rep. HMT-1, Stanford Univ., 1967.

7. Simpson, R. L.; Kays, W. M.; and Moffat, R. J.: The Turbulent Boundary Layer on a Porous Plate: An Experimental Study of the Fluid Dynamics with Injection and Suction. Rep. HMT-2, Stanford Univ., 1967.

8. Whittan, D. G.; Kays, W. M.; and Moffat, R. J.: The Turbulent Boundary Layer on a Porous Plate: Experimental Heat Transfer with Variable Suction, Blowing, and Surface Temperature. Rep. HMT-3, Stanford Univ., 1967.

9. Julien, H. L.; Kays, W. M.; and Moffat, R. J.: The Turbulent Boundary Layer on a Porous Plate: An Experimental Study of the Effects of a Favorable Pressure Gradient. Rep. HMT-4, Stanford Univ. (NASA CR-104140), Apr. 1969.

10. Thielbahr, W. H.; Kays, W. M.; and Moffat, R. J.: The Turbulent Boundary Layer on a Porous Plate: Experimental Heat Transfer with Blowing, Suction, and Favorable Pressure Gradient. Rep. HMT-5, Stanford Univ. (NASA CR-104141), Apr. 1969.

11. Tye, R. P.: An Experimental Investigation of the Thermal Conductivity and the Electrical Resistivity of Three Porous 304L Stainless Steel "Rigimesh" Materials to 1300 K. Proposed NASA CR-72710, 1970.

12. Eckert, E. R. G.; and Drake, Robert M., Jr.: Heat and Mass Transfer, Second ed., McGraw-Hill Book Co., Inc., 1959.

13. Poferl, David J.; Svehla, Roger A.; and Lewandowski, Kenneth: Thermodynamics and Transport Properties of Air and the Combustion Products of Natural Gas and of ASTM-A1 Fuel with Air. NASA TN D-5452, 1969.

14. Kreith, Frank: Principles of Heat Transfer, International Textbook Co., 1958.

15. Spalding, D. B.: A Standard Formulation of the Steady Convective Mass Transfer Problem. Int. J. Heat Mass Transfer, vol. 1, no. 2/3, 1960, pp. 192-207.

16. Mickley, H. A.; Ross, R. C.; Squyers, A. L.; and Steward, W. E.: Heat, Mass, and Momentum Transfer for Flow Over a Flat Plate With Blowing or Suction. NACA TN 3208, 1954.

17. Anon.: Engineering Properties of IN 100 Alloy. International Nickel Co., 1968.

18. Stewart, O. L.; and Vogel, W. H.: Methods for Predicting Thermal Stress Cracking in Turbine Stator or Rotor Blades. Rep. PWA-3142, Pratt & Whitney Aircraft (NASA CR-54636), July 10, 1967.

19. Kaufman, Albert: Steady-State Stress Relaxation Analysis of Turbine Blade Cooling Designs. NASA TN D-5282, 1969.

20. Kaufman, Albert: Analytical Study of Cooled Turbine Blades Considering Combined Steady-State and Transient Conditions. NASA TM X-1951, 1970.

21. Nealy, David A.: An Approximate Treatment of Heat Transfer in Plane Laminar and Turbulent Flows Over Arbitrary Surfaces with Arbitrary Surface Injection Including Wall Conduction Effects. Ph.D. Thesis, Purdue University, 1968.

22. Green, Leon, Jr.; and Duwez, Pol: Fluid Flow Through Porous Metal. J. Appl. Mech., vol. 18, no. 1, 1951, pp. 39-45.

23. Koh, J. C. Y.; and delCasal, E.: Heat and Mass Flow Through Porous Matrices for Transpiration Cooling. Proceedings 1965 Heat Transfer and Fluid Mechanics Institute. A. F. Charwat, ed., Stanford University Press, 1965, pp. 263-281.

24. Schneider, P. J.; and Brogan, J. J.: Temperature Response of a Transpiration-Cooled Plate. ARS J., vol. 32, no. 2, Feb. 1962, pp. 233-236.

25. Colladay, Raymond S.: Inverse Problems Related to Transient Convection in the Thermal Entrance Region Between Parallel Plates, Ph. D. Thesis, Michigan State University, 1969.

NASA-Langley, 1970 — 28 E-5669